complex coronary vasculature of the true and false lumens made precise evaluation of RCA flow difficult by conventional coronary angiography, coronary CT angiography was able to detect significant progression of the stenosis in the true coronary lumen.

Since affected vessels are usually revascularized in most cases without any insufficient coronary flow remaining, the natural clinical course of procedure-related coronary dissection has been rarely studied and reported. Therefore, a follow-up modality for patients with such a complication has not been established. However, the present case suggests that, for patients with residual dissection caused by procedures, coronary CT angiography might be considered as a first-line follow-up modality because it is less invasive (coronary angiography might cause exacerbation of the coronary dissection) and it is suitable for the accurate evaluation of vascular lumen, even in the presence of a very complex coronary vasculature of true or false lumens.

REFERENCES

1. Boyle AJ, Chan M, Dib J, Resar J. Catheter-induced coronary artery dissection: risk factors, prevention and management. J Invasive Cardiol 2006; 18: 500-3. (Review)
2. Huber MS, Mooney JF, Madison J, Mooney MR. Use of a morphologic classification to predict clinical outcome after dissection from coronary angioplasty. Am J Cardiol 1991; 68: 467-71.
3. Goldstein JA, Casserly IP, Katsiyiannis WT, Lasala JM, Taniuchi M. Aortocoronary dissection complicating a percutaneous coronary intervention. J Invasive Cardiol 2003; 15: 89-92. (Review)
4. Liu X, Tsujita K, Maehara A, *et al.* Intravascular ultrasound assessment of the incidence and predictors of edge dissections after drug-eluting stent implantation. JACC Cardiovasc Interv 2009; 2: 997-1004.

The FASEB Journal • Research Communication

IRF3 regulates cardiac fibrosis but not hypertrophy in mice during angiotensin II-induced hypertension

Kensuke Tsushima,*,† Tomoko Osawa,* Hideyuki Yanai,*,§ Akira Nakajima,* Akinori Takaoka,*,[1] Ichiro Manabe,† Yusuke Ohba,‡ Yasushi Imai,† Tadatsugu Taniguchi,*,§,[2] and Ryozo Nagai†,[2]

*Department of Immunology and †Department of Cardiovascular Medicine, Graduate School of Medicine, University of Tokyo, Tokyo, Japan; ‡Laboratory of Pathophysiology and Signal Transduction, Hokkaido University Graduate School of Medicine, Sapporo, Japan; and §Core Research for Evolution Science and Technology, Japan Science and Technology Agency, Tokyo, Japan

ABSTRACT **Hypertension is a typical modern life-style-related disease that is closely associated with the development of cardiovascular disorders. Elevation of angiotensin II (ANG II) is one of several critical factors for hypertension and heart failure; however, the mechanisms underlying the ANG II-mediated pathogenesis are still poorly understood. Here, we show that ANG II-mediated cardiac fibrosis, but not hypertrophy, is regulated by interferon regulatory factor 3 (IRF3), which until now has been exclusively studied in the innate immune system. In a ANG II-infusion mouse model (3.0 mg/kg/d), we compared IRF3-deficient mice ($Irf3^{-/-}/Bcl2l12^{-/-}$) with matched wild-type (WT) controls. The development of cardiac fibrosis [3.95±0.62% (WT) *vs.* 1.41±0.46% ($Irf3^{-/-}/Bcl2l12^{-/-}$); $P<0.01$] and accompanied reduction in left ventricle end-diastolic dimension [2.89±0.10 mm (WT) *vs.* 3.51±0.15 mm ($Irf3^{-/-}/Bcl2l12^{-/-}$); $P=0.012$] are strongly suppressed in $Irf3^{-/-}/Bcl2l12^{-/-}$ mice, whereas hypertrophy still develops. Further, we provide evidence for the activation of IRF3 by ANG II signaling in mouse cardiac fibroblasts. Unlike the activation of IRF3 by innate immune receptors, IRF3 activation by ANG II is unique in that it is activated through the canonical ERK signaling pathway. Thus, our present study reveals a hitherto unrecognized function of IRF3 in cardiac remodeling, providing new insight into the progression of hypertension-induced cardiac pathogenesis.—Tsushima, K., Osawa, T., Yanai, H., Nakajima, A., Takaoka, A., Manabe, I., Ohba, Y., Imai, Y., Taniguchi, T., Nagai, R. IRF3 regulates cardiac fibrosis but not hypertrophy in mice during angiotensin II-induced hypertension. *FASEB J.* 25, 1531–1543 (2011). www.fasebj.org**

Key Words: cardiac remodeling · inflammation · heart failure

CONGESTIVE HEART FAILURE (CHF) is a chronic, costly, and often fatal cardiac-related illness that is most frequently caused by hypertension (1). Hypertension-mediated excessive overload to the left ventricle (LV) causes cardiac remodeling, which includes concurrent myocyte hypertrophy and interstitial fibrosis. In the early stage of hypertension-induced pathogenesis, cardiac remodeling is considered to be an important adaptive response to maintain cardiac output (2, 3). Indeed, an increased LV wall stress is compensated for by an increased contractility of cardiac myocytes, leading to myocyte hypertrophy and LV wall thickening. In addition, an increase in tensile stress from interstitial fibrosis prevents ventricular deformation by transmitting the force generated by hypertrophied myocytes to the entire ventricle. In the later stages of cardiac remodeling, however, excessive mechanical load in myocardium leads to myocyte loss and replacement with fibrosis, which is responsible for increased myocardial stiffness and decreased pumping capacity. Consequently, a prolonged overload of the LV leads to the breakdown of these compensatory mechanisms, leading to CHF (2, 3).

Angiotensin II (ANG II) is a vasopressor, octapeptide hormone intermediate of the renin-angiotensin system (RAS) that has received much attention as a critical factor in the development of hypertension and heart failure. Normally, the RAS is activated to increase blood pressure in response to hypotension, decreased sodium concentration in the distal tubule of the kidney nephron, decreased blood volume, and renal sympathetic nerve stimulation. However, in conditions of cardiac pathogenesis, ANG II levels increase as a result of the aberrant production of ANG II-forming serine

[1] Current address: Division of Signaling in Cancer and Immunology, Institute for Genetic Medicine, Hokkaido University, Sapporo, Japan.

[2] Correspondence: T.T., Department of Immunology, Graduate School of Medicine and Faculty of Medicine, University of Tokyo, Hongo 7-3-1, Bunkyo-ku, Tokyo 113-0033, Japan. E-mail: tada@m.u-tokyo.ac.jp; R.N., Department of Cardiovascular Medicine, Graduate School of Medicine, University of Tokyo, Hongo 7-3-1, Bunkyo-ku, Tokyo 113-8655, Japan. E-mail: nagai-tky@umin.ac.jp

doi: 10.1096/fj.10-174615

This article includes supplemental data. Please visit *http://www.fasebj.org* to obtain this information.

0892-6638/11/0025-1531 © FASEB

protease, angiotensin-converting enzyme, and chymase by cardiac myocytes and mast cells, thereby causing cardiac remodeling (4, 5). Indeed, the blockade of the ANG II type I receptor not only decreases blood pressure but also markedly improves the prognosis of patients with CHF by inhibiting cardiac remodeling (6–8). In addition to its role as a vasopressor during cardiac remodeling, ANG II is reported to have pleiotropic functions including proinflammatory activity (9–11). The immune system, in general, plays an important role in CHF, as immune cells are present in hypertrophied or dilated cardiac tissues, while high levels of serum C-reactive protein and IL-6 correlate with increased mortality in patients with CHF (12, 13). Under these conditions, ANG II has a critical role in stimulating the production of reactive oxygen species and the activation of inflammatory response in the cardiovascular system (9). Despite the growing prevalence of anti-ANG II therapies, the molecular mechanisms underlying ANG II-mediated cardiac remodeling and inflammation remain poorly understood.

Interferon regulatory factor (IRF) 3 belongs to a family of transcription factors that is best known for its role in the induction of innate immune responses (14, 15). On activation of pathogen recognition receptors such as Toll-like receptors and cytosolic receptors, latent IRF3 is phosphorylated on its carboxyl terminus serine and threonine residues by TBK1 and IKKe kinases, resulting in the formation of IRF3 homodimers, nuclear translocation, and association with p300/CBP coactivators (16, 17). Activated IRF3 induces transcription of proinflammatory cytokine, type I interferon (IFN), and other genes (18–22). To date, little is known about the function of IRF3 beyond its role in the regulation of the immune system.

In the present study, we evaluated potential roles for IRFs in the regulation of the cardiovascular system and found that ANG II-mediated fibrosis is regulated by IRF3, thereby placing this IRF member in a new context. We provide evidence that IRF3 is indeed critical for the development of cardiac fibrosis, accompanied by shrinkage of the left ventricle, but not to the development of cardiac hypertrophy. We also present a novel mechanism involving the ANG II-ERK signaling pathway in the activation of IRF3, a pathway distinct from that of IRF3 activation by the receptors of the innate immune system. We discuss our results in terms of their effect in understanding hypertension-induced cardiac fibrosis and hypertrophy during CHF progression.

MATERIALS AND METHODS

Mice

Irf3$^{-/-}$*/Bcl2L12*$^{-/-}$, *Irf7*$^{-/-}$, *Pkr*$^{-/-}$, and *Ifnar1*$^{-/-}$ mice have been described previously and were maintained in specific pathogen-free conditions at the animal facility of University of Tokyo (20, 23, 24). All mice were used after backcrossing with C57BL/6J mice for ≥7 generations. C57BL/6J mice (CLEA Japan, Inc., Tokyo, Japan) served as wild-type (WT) controls. C57BL/6 Ly 5.1-Pep3b mice were purchased from B&K Universal (Hull, UK).

ANG II infusion and bone marrow (BM) transplantation

Seven- to 10-wk-old mice were used for ANG II infusion experiments. After anesthetization, an osmotic minipump (Alzet model 2002; Alza Corp., Moutain View, CA, USA) containing [Val5]-ANG II (Wako, Osaka, Japan) dissolved in 0.15 M NaCl and 10 mM acetic acid was implanted subcutaneously. Thereafter, [Val5]-ANG II was delivered at 3.0 mg/kg/d for the indicated period. Blood pressure was monitored before and after infusion (BP-98A; Softron, Tokyo, Japan). BM transplantation has been described already (25). Briefly, 6-wk-old male mice were X-ray irradiated (8.0–9.0 Gy), and then 5×10^6 BM cells were infused intravenously. At 4 wk after irradiation, the substitution rate of peripheral lymphocyte was assessed by flow cytometry, and an osmotic minipump was implanted.

Histological analysis

After intravenous injection of 150 mM KCl, hearts were immediately excised and fixed in 4% paraformaldehyde, and then they were embedded in paraffin. Transverse sections of heart were sectioned every 200 μm at the papillary muscle level and then Masson-trichrome stained. The ratio of perivascular fibrosis to lumen area was measured in coronary arteries. The ratio of interstitial fibrosis to myocardium was quantified by ImageJ software (U.S. National Institutes of Health, Bethesda, MD, USA). The value of each mouse was given as the mean value from 5 sections. Silver-stained semithin sections were used for measurement of cardiomyocyte cross-sectional area. Suitable cross-sections were defined as having round to oval cardiomyocyte sections. For immunohistochemistry of CD45, TGFβ, and αSMA, frozen sections (5–10 μm thick) were fixed in chilled acetone for 5 min. Each protein was stained using antibody for CD45 (clone 30F11 diluted 1:100; BD Pharmingen, San Diego, CA, USA), TGFβ (clone D-12 diluted 1:50; Santa Cruz Biotechnology, Santa Cruz, CA, USA), and α-SMA (clone 1A4 diluted 1:1000; Sigma, St. Louis, MO, USA). For immunohistochemistry of proliferation cell nuclear antigen (PCNA), paraffin-embedded section was pretreated with microwave for 20 min in distilled water and stained using anti-PCNA antibody (clone PC10 prediluted antibody; Dako, Copenhagen, Denmark) and Dako EnVision+ System-HRP(DAB).

Echocardiographic examination

Mice were anesthetized by intraperitoneal injection of a mixture of ketamine (48 mg/kg) and xylazine (6 mg/kg). At 10 to 20 min after peritoneal injection, cardiac function was evaluated 3 times with echocardiography (Sonos 4500; Philips, Eindhoven, The Netherlands) using a 12-MHz transducer. Cardiac function in each mouse was given as the mean value of 3 measurements.

cDNA construct

Hemagglutinin (HA)-tagged mouse AT1a receptor construct and HEK293T cells expressing mAT1a receptor (AT1-293T) were a kind gift from Dr. A. Fukamizu (Tsukuba University, Tsukuba, Japan). HA-tagged murine IRF3 was subcloned into the *Eco*RI site of pcDNA3.1(−). C1B-luc construct was a kind gift from Dr. T. Fujita (Kyoto University, Kyoto, Japan).

pGL4-CXCL10 was generated as described previously (26). RasV12 expression vector was a kind gift from Dr. M. Matsuda (Kyoto University, Kyoto, Japan). pFC-MEKK was obtained from Stratagene (La Jolla, CA, USA).

Cell culture

Primary cultures of cardiac fibroblasts were prepared from the ventricles of 1-d-old ICR mice as described previously (27). AT1-293T cells were cultured in DMEM with 10% serum. cDNAs were transfected by FuGene 6 (Roche, Indianapolis, IN, USA) according to the manufacturer's instruction. Newcastle disease virus (NDV) infection of cardiac fibroblast was performed at a concentration of 25 hemagglutinin units/1 $\times$ 10^6 cells.

Western blot analysis

Anti-IRF3 antibody and anti-hemagglutinin antibody (12CA5) were obtained from Zymed (Burlingame, CA, USA) and Roche, respectively. Anti-USF2 and anti-β-tubulin antibodies were purchased from Santa Cruz Biotechnology. Cytosolic and nuclear fractions were prepared as described previously (21). For SDS-PAGE, 5 μg of cytosol extracts and 10 μg of nuclear extracts were subjected to electrophoresis on 7.5% polyacrylamide gel as described previously (22). For native-PAGE, 7.5% polyacrylamide gel without SDS was prerun with running buffer (25 mM Tris-HCl, pH 8.4, and 192 mM glycine, with or without 0.2% deoxycholate at the cathode and anode, respectively) at 45 mA for 30 min. The sample was mixed with loading buffer (125 mM Tris-HCl, pH 6.8; 30% glycerol; and 0.002% bromphenol blue) and applied to the gel. The samples were electrophoresed at 25 mA for 50 min at 4°C (21).

Calf intestine alkaline phosphatase (CIAP) treatment

The nuclear fraction of AT1-293T cells expressing HA-IRF3 (5 μg) was treated with or without 1 U of CIAP (TaKaRa Bio Inc., Shiga, Japan) and incubated for 30 min at 37°C.

Reporter assay

AT1-293T cells were transfected by FuGene 6 (Roche) lipofection reagent. Serum-free medium was replaced 3 h after transfection and subsequently stimulated by ANG II (1 μM). Luciferase activity was assayed 14 h after ANG II stimulation. All data are expressed as means ± SD (n=4).

RNA analysis

Total RNA was prepared using Sepasol Super II (Nacalai Tesque, Kyoto, Japan). GeneChip analysis was performed by TaKaRa Bio Inc. using Affymetrix Mouse Genome 430 2.0 Array (Affymetrix, Santa Clara, CA). Quantitative real-time RT-PCR analysis was performed using LightCycler and SYBRGreen system (Roche). Data were normalized by the level of GAPDH expression in each sample. Primers used in this study are as follows: GAPDH, forward 5′-AGAACATCATCCCTGCATCC-3′ and reverse 5′-CACATTGGGGGTAGGAACAC-3′; brain natriuretic peptide (BNP), forward 5′-AGGTGCTGTCCCAGATGATT-3′ and reverse 5′-CCTTGGTCCTTCAAGAGCTG-3′; α-myosin heavy chain (αMHC), forward 5′-CAGAGGAGAAGGCTGGTGTC-3′ and reverse 5′-CTGCCCCTTGGTGACATACT-3′; procollagen type Ia1, forward 5′-GAGCGGAGAGTACTGGATCG-3′ and reverse 5′-GCTTCTTTTCCTTGGGGTTC-3′; MCP5/Ccl12, forward 5′-TCCTCAGGTATTGGCTGGAC-3′ and reverse 5′-TGGCTGCTTGTGATTCTCCT-3′; Cxcl1, forward 5′-TGTTGTGCGAAAAGAAGTGC-3′ and reverse 5′-TACAAACACAGCCTCCCACA-3′; IP10/Cxcl10, forward 5′-CGTCATTTTCTGCCTCATCCT-3′ and reverse 5′-TGGTCTTAGATTCCGGATTCAG-3′; MIP1α/CCL3, forward 5′-GCTGTTCTTCTCTGTACCATGACA C-3′ and reverse 5′-TCAACGATGAATTGGCGTG-3′; MCP1/Ccl2, forward 5′-GCCAACTCTCACTGAAGCC-3′ and reverse 5′-GCTGGTGAATGAGTAGCAGC-3′; RANTES/Ccl5, forward 5′-GTGCCCACGTCAAGGAGTAT-3′ and reverse 5′-CCACTTCTTCTCTGGGTTG-3′; and TGFβ forward 5′-ACAATTCCTGGCGTTACCTT-3′ and reverse 5′-GTTCAGCCACTGCCGTACAAC-3′.

Statistical analysis

Differences between control and experimental groups were evaluated with unpaired 2-tailed Student's t test. Comparisons between multiple groups were performed by 1-way ANOVA followed by the Fisher's protected least significant difference test for comparison of means. We considered a value of $P < 0.05$ to be significant.

RESULTS

ANG II-induced cardiac fibrosis requires IRF3

To determine whether IRFs or type I IFN responses contribute to hypertension-related cardiac remodeling, we challenged WT and IRF- and IFN signaling-deficient mice to a well-established, osmotic minipump-mediated ANG II infusion protocol (ref. 28; Supplemental Fig. S1*A*). As reported previously, ANG II causes an increase in blood pressure, ventricular weight to body weight ratio (VW/BW), and interstitial fibrosis in WT mice (28). Interestingly, we observed that ANG II-induced cardiac fibrosis is strongly suppressed in mice deficient in IRF3 and Bcl2-like-12 (Bcl2L12; *Irf3*$^{-/-}$/*Bcl2l12*$^{-/-}$ mice: as described below, these mice carry additional nullizygosity for *Bcl2l12*$^{-/-}$ gene; ref. 29) as compared with WT mice (**Fig. 1*A***). Interstitial and perivascular fibrosis in *Irf3*$^{-/-}$/*Bcl2l12*$^{-/-}$ mice is significantly attenuated, although an increase in blood pressure and VW/BW is normal (Fig. 1*A*, *B* and **Table 1**). On the other hand, no such suppression was observed in mice deficient in IRF7, another transcription factor that is known to be critical to induce type I IFN gene response (refs. 18, 20; Supplemental Fig. S1*B*).

Because IRF3 is activated by stimulation of innate immune receptors and directly regulates type I IFN gene expression (18, 20), we next examined whether type I IFN signaling is involved in ANG II-induced fibrosis. We found that cardiac fibrosis is induced by ANG II infusion in mice lacking the IFN type I receptor component IFNAR1 (*Ifnar1*$^{-/-}$ mice) or double-stranded RNA-dependent protein kinase (PKR), a well-known target gene of type I IFN signaling (*Pkr*$^{-/-}$mice; Supplemental Fig. S1*B*). Thus, a role for type I IFN signaling in the IRF3-mediated suppression of cardiac fibrosis can be excluded. These observations demonstrate a new role for IRF3, independent of its regulation of type I IFN responses, in hypertension-induced cardiac fibrosis. Note that the ANG II-induced elevation of

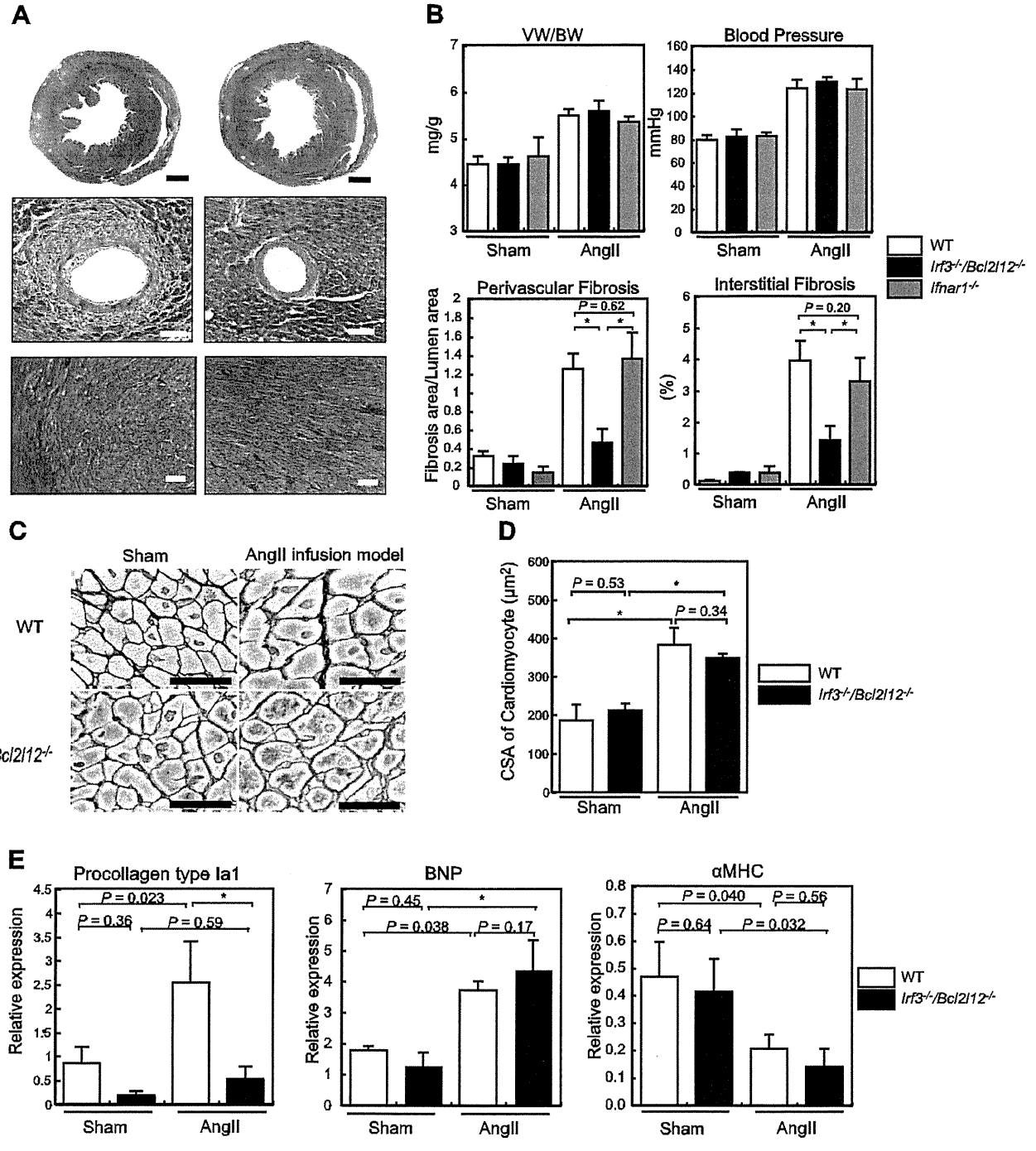

Figure 1. Cardiac fibrosis induced by ANG II is reduced in *Irf3*$^{-/-}$*/Bcl2l12*$^{-/-}$ mice. *A*) Masson-trichrome staining of transverse section of heart 14 d after ANG II infusion (3.0 mg/kg/d). Representative samples are shown in each group. *B*) Quantitative analysis of mean blood pressure, VW/BW, area of perivascular fibrosis (fibrosis area/lumen area), and interstitial fibrosis. *C*) Silver staining of transverse sections of papillary muscle after ANG II infusion. *D*) Quantification of cross-sectional area (CSA) of cardiomyocyte. There was no significant difference between WT and *Irf3*$^{-/-}$*/Bcl2l12*$^{-/-}$ mice (n=4/group). *E*) Profiling of gene expression 7 d after ANG II infusion. Expression levels of molecular markers for heart failure (BNP and αMHC) and fibrosis (procollagen type Ia1) were examined (n=3–5/group). Scale bars = 500 μm (*A*, black); 50 μm (*A*, yellow); 20 μm (*C*). Error bars = SE. *$P < 0.01$.

cardiac weight and myocyte hypertrophy are not affected by the deficiency of IRF3 (Fig. 1*B–D* and Table 1), suggesting a hitherto unrecognized dissociation of the 2 events that are critical to cardiac hypertrophy.

We also examined gene expressions of molecular markers for heart failure (BNP and αMHC and fibrosis (procollagen type Ia1) in the heart by quantitative RT-PCR (Fig. 1*E*). Consistent with histological findings, the expression level of procollagen type Ia1 was significantly decreased in *Irf3*$^{-/-}$*/Bcl2l12*$^{-/-}$ hearts compared with WT control,

TABLE 1. *Quantitative analysis of mean blood pressure, VW/BW, area of perivascular fibrosis (fibrosis area/lumen area), and interstitial fibrosis after ANG II infusion*

	Wild		*Irf3*$^{-/-}$/*Bcl2l12*$^{-/-}$		*Ifnar1*$^{-/-}$	
Parameter	Sham	ANG II	Sham	ANG II	Sham	ANG II
Mice (*n*)	6	9	6	9	3	4
BP (mmHg)	79.6 ± 4.0	124.2 ± 7.2	82.4 ± 6.4	129.4 ± 4.0	82.9 ± 2.8	123.0 ± 8.8
VW (mg)/BW (g)	4.45 ± 0.17	5.50 ± 0.13	4.45 ± 0.14	5.59 ± 0.22	4.61 ± 0.42	5.36 ± 0.12
Perivascular fibrosis	0.32 ± 0.05	1.26 ± 0.16	0.23 ± 0.09	0.46 ± 0.15*	0.14 ± 0.07	1.37 ± 0.28
Interstitial fibrosis (%)	0.10 ± 0.03	3.95 ± 0.62	0.38 ± 0.01	1.41 ± 0.46*	0.36 ± 0.21	3.30 ± 0.74

Values are means ± SE. BP, blood pressure. *$P < 0.05$ *vs.* WT control.

despite that the expression patterns of BNP and αMHC were not different between WT and *Irf3*$^{-/-}$/*Bcl2l12*$^{-/-}$ hearts.

Since the mutant mice carry another nullizygocity other than *Irf3*, *i.e.*, *Bcl2l12* gene (29), we examined whether apoptosis of cardiomyocytes is affected by the absence of Bcl2L12. As shown in **Fig. 2*A***, TUNEL$^+$ cells were mainly localized in the interstitial fibrotic area, and we could not detect TUNEL$^+$ cells in troponin T$^+$ cardiomyocytes, suggesting that cells other than cardiomyocytes undergo apoptosis, which occur in independently of Bcl2L12. Induction of apoptosis in isolated adult cardiac fibroblast by hydrogen peroxide (H_2O_2), which represent the ANG II-induced oxidative stress (30, 31), was also unaffected by the absence of Bcl2L12 (Fig. 2*B*). Furthermore, immunostaining for PCNA revealed that the proliferation of cardiac cells did not differ between 2 groups (Fig. 2*C*). These results *in toto* suggest that the involvemenat of Bcl2L12 in cardiac fibrosis is little if any.

Selective contribution of IRF3-mediated fibrosis to physiological cardiac functions

To evaluate further the pathological consequences of the above observations, we next examined cardiac function *in vivo* by transthoracic echocardiography. As shown in Fig. 2 and **Table 2**, the LV wall becomes significantly thicker in WT mice (1.5-fold increase) and

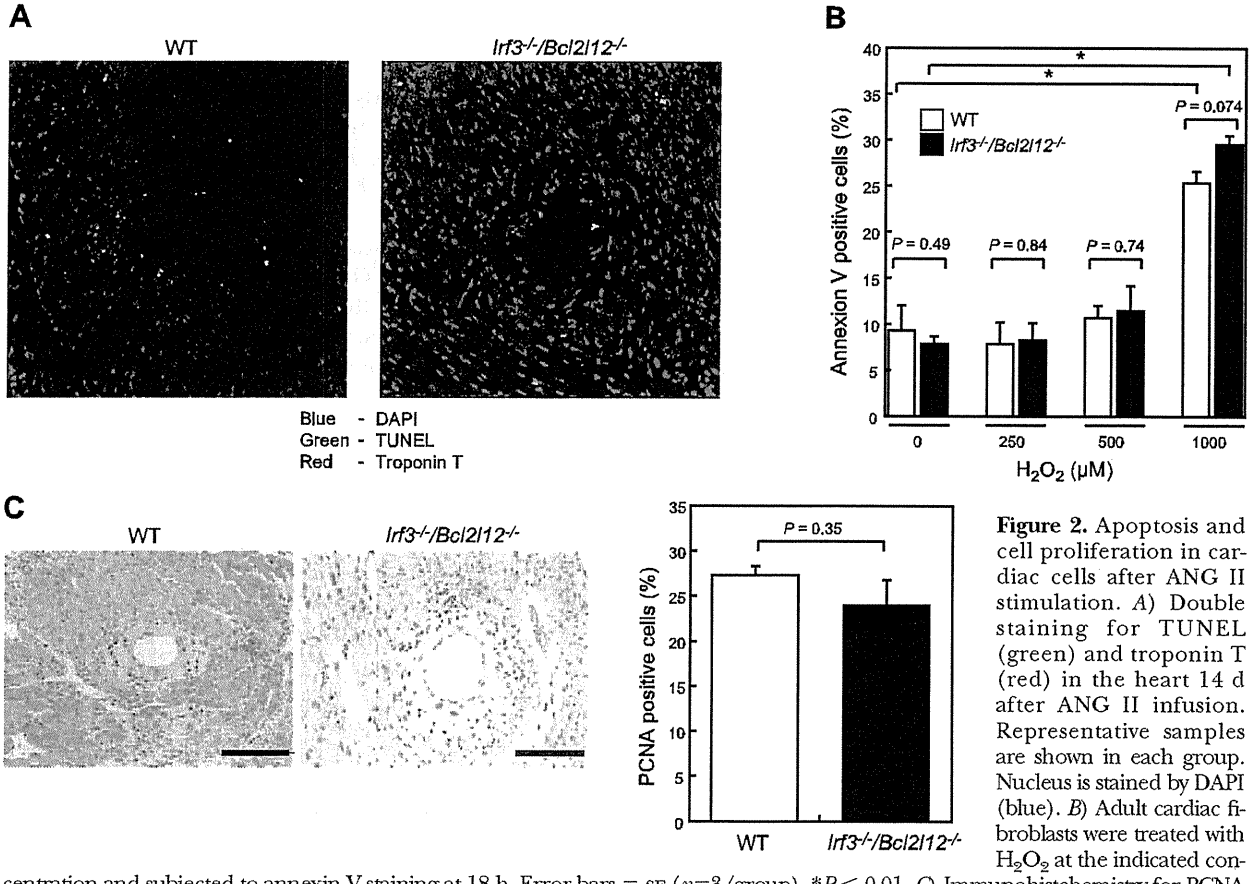

Figure 2. Apoptosis and cell proliferation in cardiac cells after ANG II stimulation. *A*) Double staining for TUNEL (green) and troponin T (red) in the heart 14 d after ANG II infusion. Representative samples are shown in each group. Nucleus is stained by DAPI (blue). *B*) Adult cardiac fibroblasts were treated with H_2O_2 at the indicated concentration and subjected to annexin V staining at 18 h. Error bars = SE (n=3/group). *$P < 0.01$. *C*) Immunohistchemistry for PCNA in the heart from ANG II-treated mice and the quantification of PCNA$^+$ cells (n=3/group). Scale bars = 100 μm.

TABLE 2. *Echocardiographic measurements*

Parameter	WT		*Irf3*$^{-/-}$	
	Pretreatment	Post-treatment	Pretreatment	Post-treatment
Mice (*n*)	8	8	9	9
BW (g)	26.2 ± 0.55	21.7 ± 0.29*	26.0 ± 0.43	22.4 ± 0.70*
HR (beats/min)	317 ± 7.68	306 ± 11.6	325 ± 14.1	307 ± 13.9
LVDd (mm)	3.42 ± 0.07	2.89 ± 0.10*	3.68 ± 0.17	3.51 ± 0.15#
LVDs (mm)	2.36 ± 0.05	1.87 ± 0.08*	2.57 ± 0.15	2.59 ± 0.15#
FS	0.31 ± 0.01	0.35 ± 0.01*	0.30 ± 0.02	0.26 ± 0.02#
IVSth (mm)	0.77 ± 0.02	1.16 ± 0.04*	0.75 ± 0.01	1.05 ± 0.03*
PWth (mm)	0.77 ± 0.03	1.10 ± 0.04*	0.76 ± 0.02	1.02 ± 0.02*
LV mass (mg)	82.0 ± 4.13	113 ± 6.25*	95.3 ± 9.52	136 ± 12.0*

Values are means ± SE. Echocardiographic and BW measurements were performed sequentially before and after ANG II infusion. HR, heart rate; LVDd, left ventricular end-diastolic diameter; LVDs, left ventricular end-systolic diameter; FS, fractional shortening; PWth, left ventricular posterior wall thickness in end diastole; IVSth, interventricular septum thickness in end diastole. *$P < 0.05$ *vs.* pretreatment; #$P < 0.05$ *vs.* WT post-treatment.

Irf3$^{-/-}$/*Bcl2l12*$^{-/-}$ mice (1.4-fold increase) after ANG II infusion. In WT mice, we observed a significant decrease in the LV end-diastolic diameter (LVDd; 1.2-fold decrease) accompanied with an increase in fractional shortening (FS; 1.1-fold increase), which is a consequence of compensation for reduced LV volume (32). Interestingly, however, these changes in FS and LVDd were not significant in *Irf3*$^{-/-}$/*Bcl2l12*$^{-/-}$ mice, although there was a trend for decrease in FS of *Irf3*$^{-/-}$/*Bcl2l12*$^{-/-}$ mice after ANG II infusion (**Fig. 3** and Table 2). These observations are consistent with the dissociation between fibrosis and hypertrophy (Fig. 1*A–D;* refs. 3, 33).

Gene expression profiles in ANG II-treated hearts

The above observations prompted us to next examine what kind of genes are affected by the absence of IRF3. We performed a genome-wide screen of mRNA in heart tissue of WT and *Irf3*$^{-/-}$/*Bcl2l12*$^{-/-}$ mice with or without ANG II infusion. ANG II infusion affected the expression of 16.9% of the genes on d 4 in WT mice (significance cutoff of 1.5-fold; Supplemental Fig. S2*A*). Since IRF3 is known to regulate a variety of chemokine genes (14), we listed the expression profile of chemokines and revealed that the expression of mRNA, such as *Cxcl10, Ccl12,* and *Cxcl1,* is decreased in *Irf3*$^{-/-}$/*Bcl2l12*$^{-/-}$ mice (Supplemental Fig. S2*B*). We confirmed that *Cxcl10, Ccl12,* and *Cxcl1* gene expressions are ANG II-IRF3 dependent by quantitative RT-PCR (**Fig. 4*A***); it is known that the *Cxcl10* gene is also activated by IRF3 through signaling by innate immune receptors (14, 34). The presence of IRF binding sites [IFN-stimulated response element (ISRE)] was confirmed in the promoter region of *Ccl12* gene (data not shown); this IRF3-dependent Ccl12 gene induction by ANG II is particularly interesting because of the report showing that Ccl12 neutralization significantly protects fibrosis formation by inhibiting fibrocyte recruitment in the mouse model of FITC- or bleomycin-induced pulmonary fibrosis (35).

In ANG II-mediated pathogenesis, interrelation between ANG II and TGFβ is established (36, 37). We also examined whether the expression of TGFβ might be decreased in the heart of *Irf3*$^{-/-}$/*Bcl2l12*$^{-/-}$ mice after ANG II infusion. Quantitative RT-PCR analysis revealed that mRNA expression in the ventricle was not different

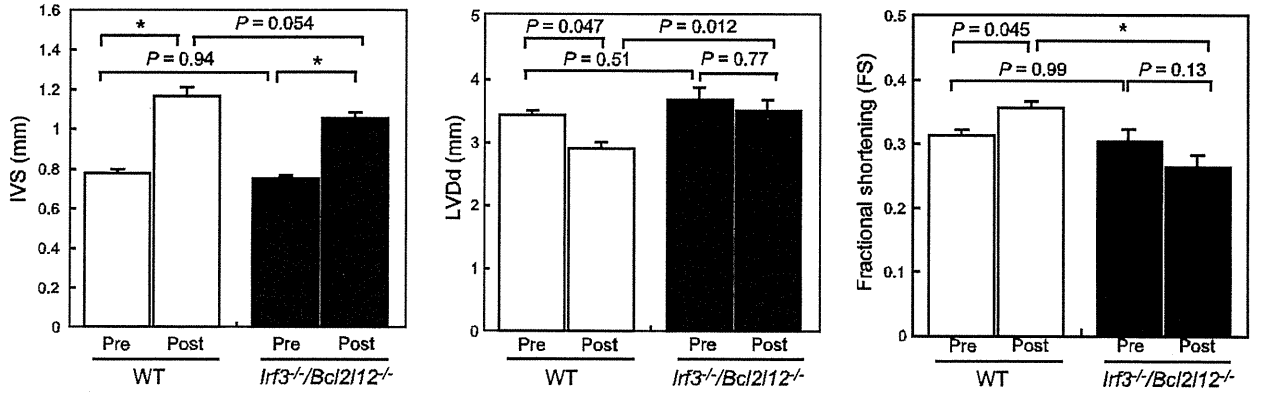

Figure 3. Echocardiographic analysis. Reduction in LVDd after ANG II infusion was strongly suppressed in *Irf3*$^{-/-}$/*Bcl2l12*$^{-/-}$ mice. Changes in interventricular septum (IVS), LVDd, and FS by ANG II infusion model. Error bars indicate SE (n=8–9). *$P < 0.01$.

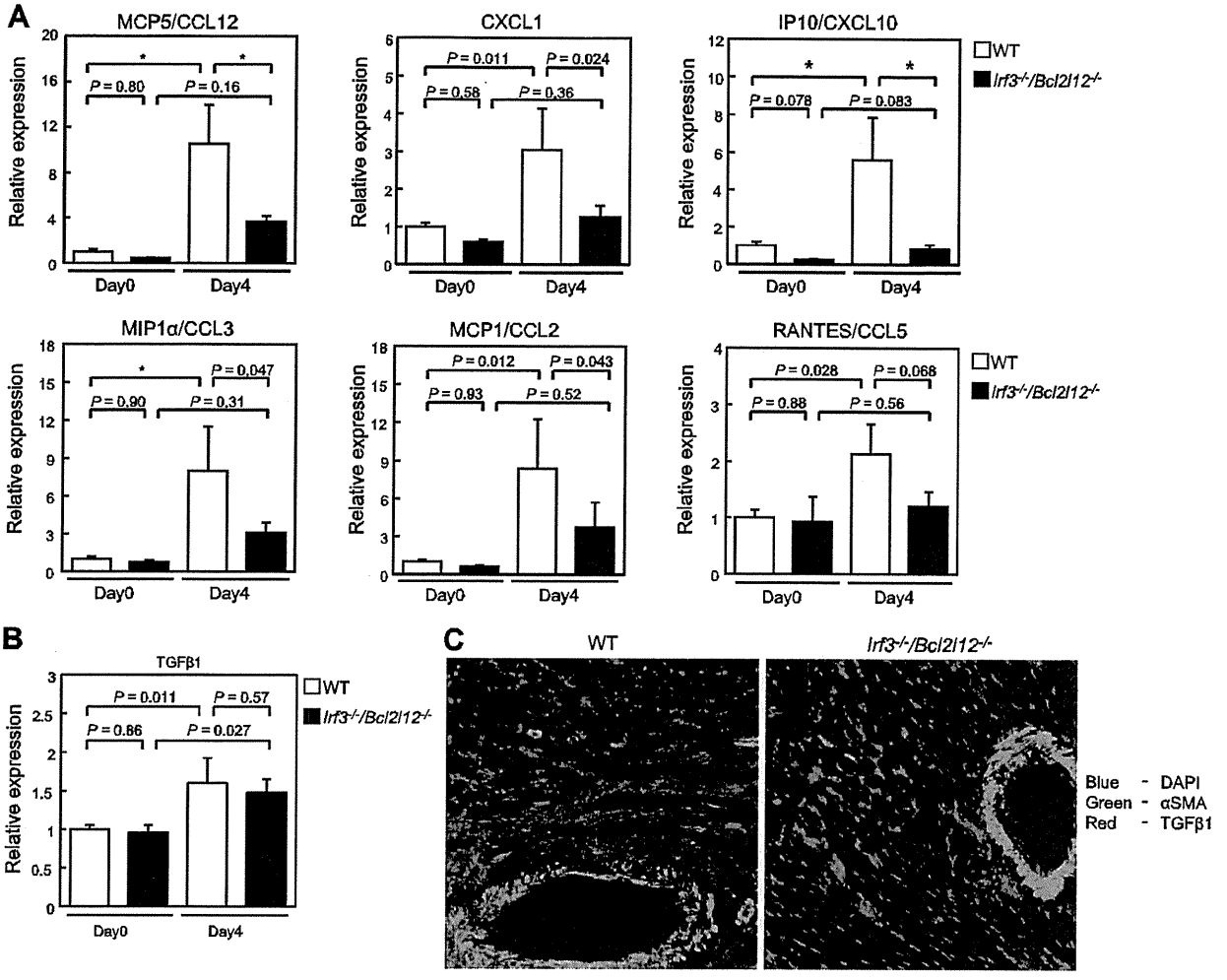

Figure 4. Chemokine and TGFβ expression in ANG II-treated heart. *A*) Expression of chemokine mRNA analyzed by quantitative RT-PCR. *B*) Expression of TGFβ mRNA analyzed by quantitative RT-PCR. *C*) Immunohistochemistry for TGFβ (red) and αSMA (green) in the heart after ANG II infusion for 14 d. Nucleus is stained by DAPI (blue). Error bars = SE (n=6/group). *$P < 0.01$.

between WT and *Irf3*$^{-/-}$/*Bcl2l12*$^{-/-}$ mice (Fig. 4*B*). Immunostaining for TGFβ shows that the expression was localized in the interstititum of the heart and that there was no suppression in the heart of *Irf3*$^{-/-}$/*Bcl2l12*$^{-/-}$ mice (Fig. 4*C*). The induction of TGFβ was not different between WT and *Irf3*$^{-/-}$/*Bcl2l12*$^{-/-}$ mice.

Recruitment of immune cells to ANG II-treated hearts

The decreased expression levels of chemokine genes in *Irf3*$^{-/-}$/*Bcl2l12*$^{-/-}$ hearts prompted us to investigate the recruitment efficiency of CD45$^+$ BM-derived cells after ANG II infusion. It has been proposed that hormonal factors secreted from recruited immune cells enhance the phenotypic transition and activation of fibroblasts during the process of fibrosis (38). As shown in **Fig. 5*A***, immunohistochemical analysis revealed the migration of a substantial number of CD45$^+$ cells to the perivascular and interstitial areas in ANG II-treated WT mice. By contrast, the infiltration of CD45$^+$ cells is significantly inhibited in ANG II-treated *Irf3*$^{-/-}$/*Bcl2l12*$^{-/-}$ mice (Fig. 5*A*).

These observations raise the possibility that the suppression of fibrosis in the *Irf3*$^{-/-}$/*Bcl2l12*$^{-/-}$ heart is due to a migration defect of BM-derived cells following ANG II treatment. To address this issue, we transplanted BM cells from congenic C57BL/6-Ly5.1 WT (CD45.1) mice into irradiated WT (CD45.2) or *Irf3*$^{-/-}$/*Bcl2l12*$^{-/-}$ (CD45.2) mice and then infused ANG II into the transplanted mice (Fig. 5*B*). As shown in Fig. 5*C*, no significant difference was observed in mean BP and VW/BW between WT (CD45.1) BM → *Irf3*$^{-/-}$/*Bcl2l12*$^{-/-}$ (CD45.2) chimeras and WT (CD45.1) BM → WT (CD45.2) chimeras. However, WT (CD45.1) BM → *Irf3*$^{-/-}$/*Bcl2l12*$^{-/-}$ (CD45.2) chimeras showed less severe fibrosis and inflammatory changes than WT (CD45.1) BM → WT (CD45.2) chimeras (Fig. 5*D*). These results therefore suggest that the contributions of IRF3 in cells other than immune cells, such as mesenchymal cells, including cardiomyocytes, and resident fibroblasts play the major role in ANG II-induced fibrosis. Congruent with this notion is the fact that the

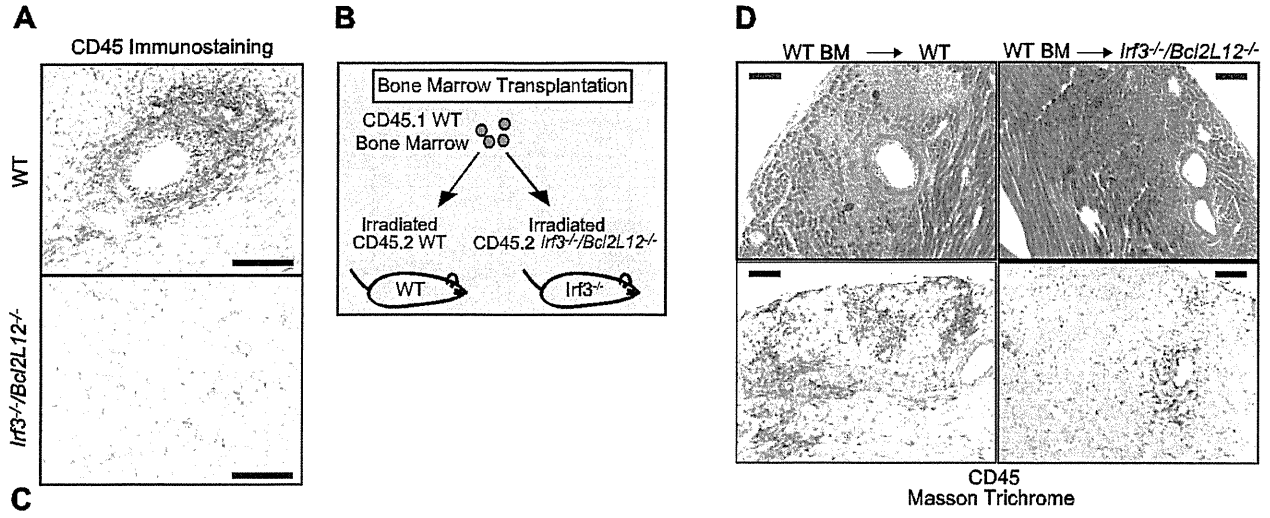

C

	WT BM → WT (n=4)	WT BM → *Irf3-/-/Bcl2L12-/-* (n=4)
mean BP (mmHg)	122.1 ± 1.92	122.4 ± 6.0
VW (mg) / BW (g)	5.67 ± 0.66	5.38 ± 0.51
Perivascular fibrosis	1.80 ± 0.12	0.61 ± 0.01*

Figure 5. Infiltration of $CD45^+$ cells in WT and $Irf3^{-/-}/Bcl2L12^{-/-}$ mice after ANG II infusion. *A*) Transverse section of heart after ANG II infusion stained by anti-CD45 antibody. $CD45^+$ cells are stained brown. *B*) Scheme of BM transplantation. Substitution rate in peripheral lymphocytes of chimeras was analyzed 4 wk after transplantation by flow cytometry. Note that the substitution rate was 82.5 ± 3.8%. *C*) Quantitative values of mean blood pressure, VW/BW, and perivascular fibrosis of chimeras after ANG II infusion. Values are means ± SE (n=4). *P = 0.014 *vs.* control group. *D*) Masson-trichrome and immunohistochemical staining of transverse sections of chimeras after ANG II infusion. Scale bars = 200 μm.

presence of the AT1a receptor in resident tissue is required for the initiation of ANG II-induced atherosclerosis (39). Although the role of IRF3 in nonhematopoietic cells is apparent, these data do not rigorously rule out that IRF3 in BM cells also contributes to the overall phenotype (see Discussion).

Distinct forms of activated IRF3 between ANG II and innate immune receptor signaling

The above observations prompted us to next examine whether IRF3 is activated by ANG II signaling. It is well established that virus infection leads to the activation of IRF3 *via* pathogen recognition receptor signaling, resulting in the activation of type I IFN genes (21, 22). We first examined the nuclear translocation of IRF3 by ANG II stimulation in cardiac fibroblasts from neonatal mice and observed nuclear translocation of IRF3 (**Fig. 6*A***). We noted that in contrast to nuclear IRF3 from cardiac fibroblasts infected by NDV, which showed a phosphorylation-induced mobility shift (21, 22), no mobility shift was observed for nuclear IRF3 induced in ANG II-stimulated cardiac fibroblasts. This observation suggests that the ANG II-mediated nuclear translocation of

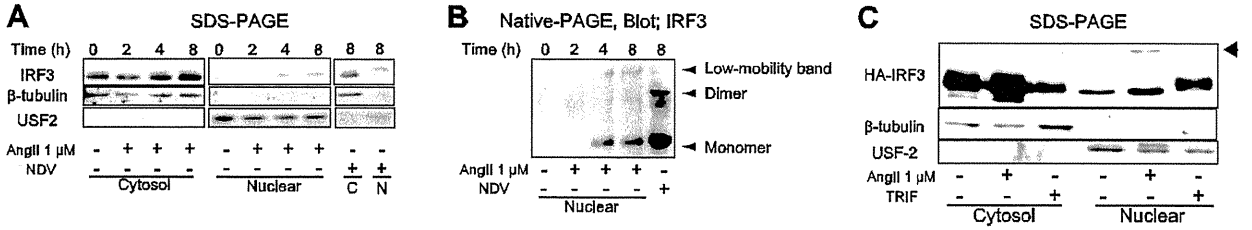

Figure 6. ANG II-induced activation of IRF3. *A*) Mouse neonatal cardiac fibroblasts were incubated in serum-free medium for 48 h and then stimulated with ANG II (1 μM). Cytosol and nuclear fractions were prepared after the stimulation for the indicated periods and were subjected to SDS-PAGE. Immunoblot analysis was performed by using anti-IRF3, anti-β-tubulin, or anti-USF2 antibody. Note that IRF3 translocated into nucleus 4 h after ANG II stimulation. NDV infection served as positive control; IRF3 shifted band was detected in the nuclear fraction. C, cytosolic fraction; N, nuclear fraction. *B*) Nuclear extract from ANG II-treated cardiac fibroblasts was subjected to native-PAGE. Immunoblot was performed using an anti-IRF3 antibody. Of note, a low-mobility band that is different from dimerized IRF3 was observed 4 h after ANG II stimulation (lanes 3 and 4; arrowhead). *C*) AT1-293T-HAIRF3 cells were stimulated with ANG II (1 μM). Cytosol and nuclear fractions were prepared 8 h after stimulation and were subjected to immunoblot analysis. As a control, cell extracts of HA-IRF3- and TRIF-expressing AT1-293T cells were analyzed. Arrowhead indicates ANG II-stimulation-specific migration of HA-IRF3.

IRF3 is mediated by a mechanism distinct from that of viral infection. Consistent with this notion, IRF3 homodimers, as detected by native-PAGE, were not observed in ANG II-stimulated cells, unlike following NDV infection. Instead, a weak intensity, low-mobility band was detected (Fig. 6*B*).

To gain further insights into the signaling pathway of ANG II-mediated IRF3 activation, we overexpressed TRIF, an adaptor protein that functions downstream of Toll-like receptor-mediated IRF3 activation (40), in HEK293T cells that stably express the murine AT1a receptor (AT1-293T; ref. 41; Supplemental Fig. S3). TRIF overexpression, however, did not induce the shifted band of nuclear IRF3 that is observed on stimulation with ANG II (Fig. 6*C*). Taken together, these findings suggest that IRF3 is activated by mechanisms distinct from the previously described pathway activated by innate immune receptors, the hallmark of which is the formation of the IRF3 homodimer.

ANG II signaling pathway critical to IRF3 activation

It is well established that on stimulation of innate immune receptors by virus or other agent, serine/threonine protein kinases, such as TBK1 and IKK, are activated, resulting in the phosphorylation of IRF3 at multiple serine and threonine residues located in the carboxyl terminus of IRF3 (16, 17, 21, 22). To further clarify whether phosphorylation is involved in the ANG II-induced activation of IRF3, nuclear IRF3 isolated from ANG II-stimulated AT1-293T cells expressing HA-IRF3 (AT1-293T-HAIRF3) were treated with CIAP and subjected to a mobility-shift assay. As shown in **Fig. 7*A*** (left panel, arrowhead), a majority of the low-mobility band, which we presume represents an active form of ANG II-induced IRF3, was shifted to a faster migrating band on CIAP treatment. As expected, the band representing nuclear IRF3 activated by TRIF expression showed a faster migration than the untreated band (Fig. 7*A*; right panel). These findings suggest that phosphorylation is critical to the ANG II signal-dependent activation of IRF3 but is mediated by kinases distinct from those activated by innate immune receptors. We examined whether additional modifications, such as ubiquitination or SUMOylation, of IRF3 are induced by ANG II signaling; however, immunoblotting analysis of the nuclear fraction of ANG II-stimulated AT1-293T-HAIRF3 cells using the antibodies for ubiquitin or SUMO revealed that none of these modifications could be detected (data not shown). Thus, in addition to phosphorylation, another as-yet unknown mechanism operates to generate this newly identified, active form of IRF3, which apparently does not involve homodimerization.

To examine the further the importance of phosphorylation in ANG II-dependent activation of IRF3, we examined the effects of inhibitors of MEK, PI3K, and p38 MAPK on IRF3 activation (42). Interestingly, the induction of the active form of IRF3 was strongly and selectively inhibited by the MEK-specific inhibitor U0126, suggesting the involvement of the Ras-ERK signaling pathway, known to be activated by ANG II stimulation (43–45), in the modification and activation of IRF3 (Fig. 7*B, C*). Consistent with this, transfection of either active form of Ha-Ras or MEK (together with ERK) resulted in the nuclear translocation of IRF3 characteristic of ANG II-induced IRF3 (Fig. 7*D*).

Transcriptional activity of IRF3 activated by ANG II-ERK pathway

We next addressed the issue of whether the above-described nuclear translocation of IRF3, mediated by

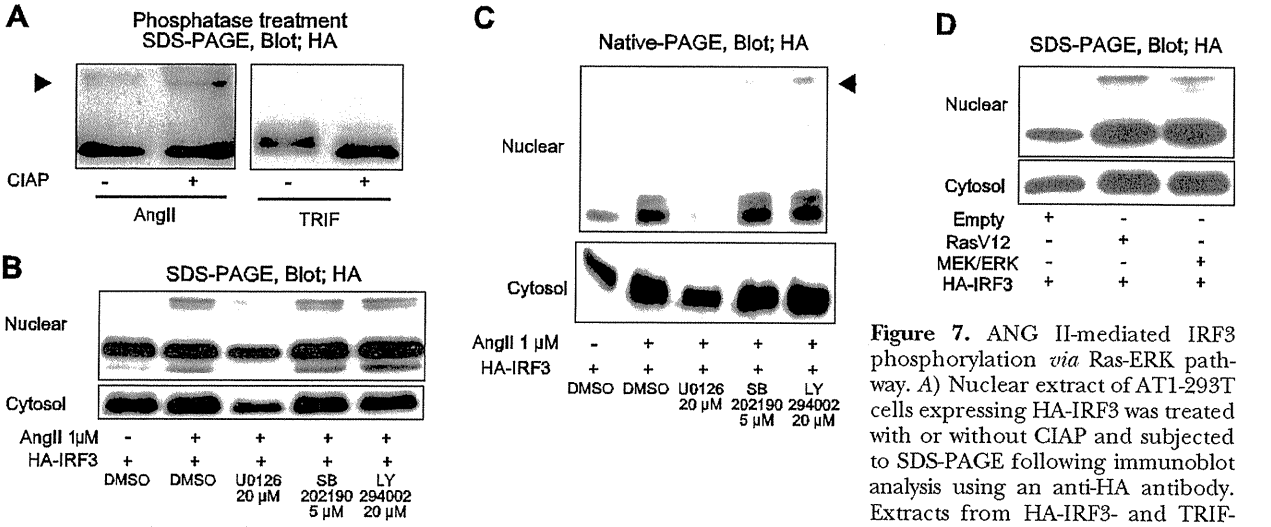

Figure 7. ANG II-mediated IRF3 phosphorylation *via* Ras-ERK pathway. *A*) Nuclear extract of AT1-293T cells expressing HA-IRF3 was treated with or without CIAP and subjected to SDS-PAGE following immunoblot analysis using an anti-HA antibody. Extracts from HA-IRF3- and TRIF-expressing AT1-293T cells were used as controls (right panel). Arrowhead indicates ANG II stimulation specific migration of HA-IRF3. *B, C*) AT1-293T cells were treated with U0126 (MEK inhibitor), SB202190 (p38 inhibitor), and LY294002 (PI3K inhibitor) for 20 min before ANG II stimulation. Extracts from nuclear and cytosol fractions were subjected to SDS-PAGE (*B*) or native-PAGE (*C*). Arrowhead indicates ANG II-specific low-mobility band (*C*). *D*) AT1-293T cells were transiently cotransfected with a combination of HA-IRF3 and constitutive active Ras (RasV12) or HA-IRF3, constitutive active MEK and ERK expression vectors. After 24 h of transfection, extracts of nuclear fraction and cytosol fraction were prepared and subjected to immunoblot analysis.

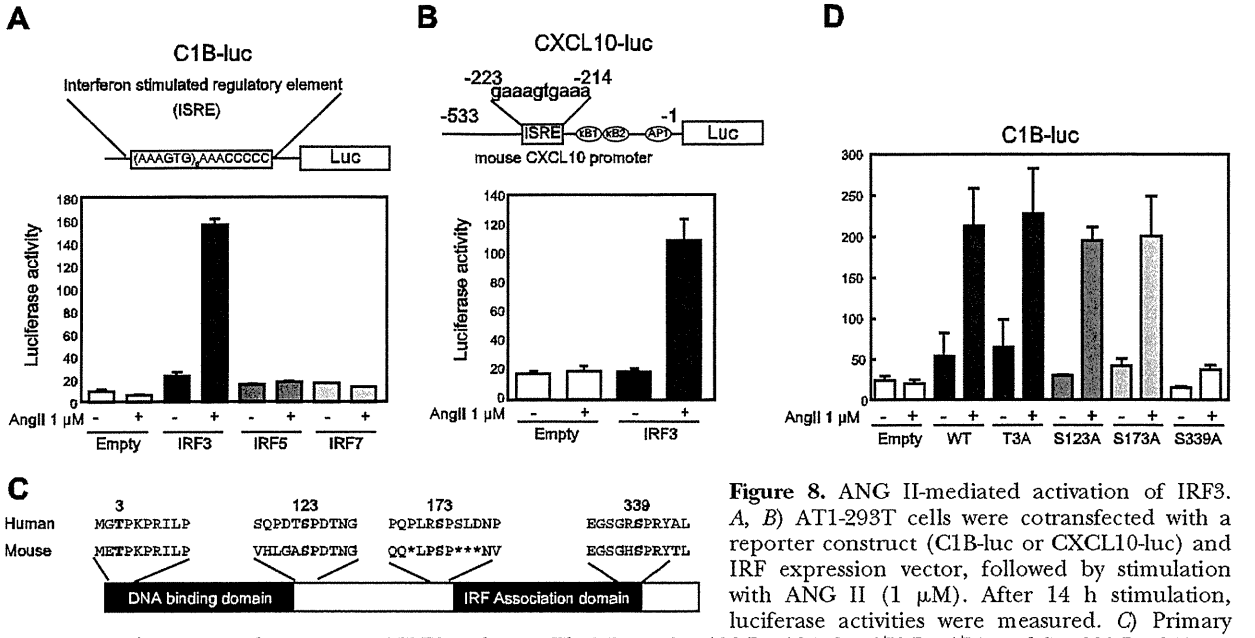

Figure 8. ANG II-mediated activation of IRF3. *A*, *B*) AT1-293T cells were cotransfected with a reporter construct (C1B-luc or CXCL10-luc) and IRF expression vector, followed by stimulation with ANG II (1 μM). After 14 h stimulation, luciferase activities were measured. *C*) Primary structure and amino acid sequence of IRF3 is shown. Thr3-Pro4, Ser-123-Pro124, Ser-173-Pro174, and Ser-339-Pro340 are conserved between human and mouse. *D*) AT1-293T cells were cotransfected with C1B-luc and wild-type IRF3 (WT) or various IRF3 mutants (T3A, S123A, S173A, and S339A) and then stimulated with ANG II (1 μM). After 14 h stimulation, luciferase activity was measured.

the ANG II-Ras-ERK signaling pathway, results in the transcriptional activation of its target sequences. To test this, we carried out a transient reporter gene assay in which the expression of a luciferase reporter gene is driven by IRF-binding sites (C1B-luc; ref. 46). As shown in **Fig. 8*A***, the cotransfection of the reporter gene with an IRF3 expression vector in AT1-293T cells resulted in the ANG II-dependent activation of the reporter gene, which presumably occurs *via* IRF3 activation without homodimer formation (Fig. 6*B*); the reporter gene activation in these cells was also observed by the overexpression of ERK or the active form of Ras without ANG II stimulation (data not shown). On the other hand, neither the expression of IRF5 nor IRF7 showed an ANG II-dependent activation of the reporter gene, further supporting the notion that ANG II signaling selectively activates IRF3 (Fig. 8*A*). Furthermore, as shown in Fig. 8*B*, this ANG II-IRF3-dependent activation was also observed using the promoter of the *Cxcl10* gene, which was induced in the heart of the ANG II-infused mice (see Fig. 4*A* and Supplemental Fig. S2*B*).

Ser-339 is critical target site for ANG II-induced activation of IRF3

ERK is a proline-directed protein kinase that phosphorylates either a Ser or Thr residue that precedes a Pro (Ser/Thr-Pro). There are 4 Ser/Thr-Pro sites (Thr3, Ser-123, Ser-173, and Ser-339) in IRF3 conserved between human and mouse. We generated mutants by site-directed alanine substitutions of each potential ERK phosphorylation site of IRF3, respectively referred to as T3A, S123A, S173A, and S339A (see Fig. 8*C*). Interestingly, the S339A mutant was found to be defective in the ANG II-induced activation of the C1B-luc reporter gene, whereas T3A, S123A, and S173A were as active as WT IRF3 (Fig. 8*D*). Consistent with these data, CXCL10 promoter activity was also decreased by >2-fold in S339A mutant-transfected cells (data not shown). Thus, Ser-339 appears to be critical for the function of IRF3 in this context. It is interesting that Ser-339 is shown to be critical for IRF3's interaction with the proryl isomerase Pin1, which results in negative regulation of type I IFN gene induction (47). We therefore addressed the issue of whether Pin1 affects ISRE activation by ANG II-activated IRF3, using the above described ANG II-induced C1B reporter gene assay, and found that reporter gene activation by ANG II was inhibited by Pin1 in a dose-dependent manner. These data suggest that Pin1 may also function as negative regulator in the ANG II signal-IRF3 pathway (data not shown; see Discussion).

DISCUSSION

In this study, we show for the first time the involvement of the IRF3 transcription factor beyond the context of its well-known function in the regulation of innate immune responses, namely, in the regulation of cardiac remodeling. Although mechanisms underlying the pathogenesis of cardiovascular remodeling have been studied in relation to chronic inflammation and immune responses (48, 49), our study provides new mechanistic insight by demonstrating ANG II-stimulated activation of IRF3 in cardiac fibroblasts, which is apparently critical to the development of cardiac fibrosis. However, it is not rigorously ruled out that IRF3 in cells of hematopoietic lineage also participate in the

development of cardiac fibrosis, perhaps as indicated by the recruitment of $CD45^+$ cells to the fibrotic heart. This will be an interesting issue to address in future studies.

Hypertrophic growth of the heart can be induced by physiological or pathological stimuli. Although both physiological and pathological hypertrophies are similar in terms of enlarged myocytes, they are mediated by distinct signaling pathway. Physiological hypertrophy is characterized by the normal organization of cardiac structure without interstitial fibrosis and a normal pattern of cardiac gene expression, which are mainly mediated by signaling through IGF1, insulin, and other growth factors. On the other hand, pathological hypertrophy is associated with both interstitial fibrosis and an altered expression pattern of contractile or calcium-handling genes (50) and is mediated by signaling mainly through G-protein-coupled receptors such as the ANG II type 1 receptor. In this regard, our current results are interesting in that only the development of interstitial fibrosis was contingent on IRF3 in ANG II-induced pathogenesis (Fig. 1*A*). To our knowledge, this is the first demonstration of the dissociation of the 2 hypertension-induced events, namely, cardiac fibrosis and hypertrophy.

While hypertrophy is IRF3 independent, the initiation of fibrosis is controlled by IRF3 indicating that ANG II initiates ≥2 different pathways (**Fig. 9**). The onset of fibrosis could be brought about by the activity of mesenchymal cells, which usually produce a specific subset of chemokines, such as Ccl12, Cxcl1, or Cxcl10, to recruit $CD45^+$ cells to the interstitium. In the absence of IRF3, the induction of these cytokines is reduced as is the migration of $CD45^+$ cells. These cells may play a role in the remodeling of the heart to adapt to increased wall tension. Indeed, the overall effect can be measured by echocardiography; we demonstrated that the contractile capacity was not increased in $Irf3^{-/-}/Bcl2l12^{-/-}$ mice (Fig. 3 and Table 2).

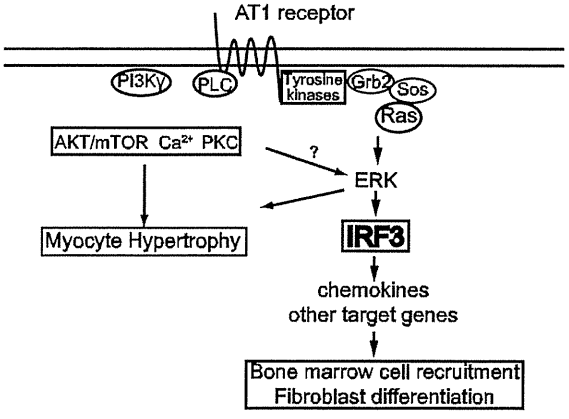

Figure 9. Schematic illustration of ANG II-mediated activation of IRF3. IRF3 is activated by Ras-ERK pathway, which is presumably initiated by tyrosine kinase activation, and this pathway is critical to the development of cardiac fibrosis. On the other hand, IRF3 activation mediated by this pathway is not linked to the ANG II-mediated caridiac hypertrophy, which may be regulated by other signaling pathways depicted in the left part of the figure.

As shown in Fig. 5*A*, a large number of $CD45^+$ cells accumulated within the fibrotic lesions of WT mice. The origins of fibroblasts in the heart are still unclear but ≥3 possibilities have been proposed: resident fibroblasts, transdifferentiation through endothelium to mesenchymal transition (EndMT; ref. 51), and BM-derived fibroblasts differentiated from $CD45^+$ cells called fibrocytes (51, 52). Indeed, we also found that myofibroblasts expressing α-smooth muscle actin in fibrosis lesions strongly colocalized with $CD45^+$ cells (data not shown). Although further investigation is required in order to discuss the function of the $CD45^+$ cells, it seems clear that signaling events in mesenchymal cells, such as ANG II-induced IRF3 activation, could result in attracting these immune cells to enhance the fibrosis event. In addition, it is not rigorously excluded that fibrogenic actions such as induction of type I and III collagens are also affected in the absence of IRF3 in cardiac fibroblasts.

We have also provided evidence for a novel mechanism of IRF3 activation. In the canonical TBK1/IKK pathway, phosphorylation-dependent modifications are crucial for regulating the function of IRF3. Indeed, IRF3 is phosphorylated by ANG II signaling *via* the Ras-ERK pathway. This is congruent with previous reports (43, 53) showing the involvement of tyrosine kinase activation and subsequent Ras activation by ANG II signaling; we infer that the activation of IRF3 is linked to this ANG II signaling pathway (Fig. 9). However, Ras-ERK-mediated activation does not produce the subsequent dimer formation or hyperphosphorylated form of IRF3 that is induced by innate immune receptor signaling. Unexpectedly, we discovered a novel low-mobility band of IRF3, which is different from the well-established activated form of IRF3. Moreover, our study, which employed a reporter assay, indicates a critical role of Ser-339 of IRF3 in its ANG II-mediated activation; however, whether Ser-339 is directly activated by ERK kinases remains to be clarified. According to our preliminary data, obtained from *in vitro* phosphorylation assay, ANG II-activated ERK2 can phosphorylate both recombinant IRF3-WT and IRF3-S339A; therefore, it is likely that ERK may directly phosphorylate Ser-339 and other sites of IRF3 following ANG II stimulation (data not shown).

Interestingly, the phosphorylation of Ser-339 results in the negative regulation of IRF3 when activated by innate immune receptors *via* the recruitment of PinI, which suppresses type I IFN responses (47). Thus, one may envisage a dual function of Ser-339, in which Ser-339 either can serve in the activation of IRF3 during ANG II signaling or negatively regulate IRF3 by recruiting PinI following innate immune receptor signaling. Nevertheless, it remains to be rigorously clarified whether ANG II-Ras-ERK directly targets IRF3 and, if so, whether it is sufficient for IRF3 activation. Moreover, the molecular nature of nuclear-translocated IRF3, which is apparently distinct from the IRF3 ho-

modimer formed on viral infection, is undefined. To understand this unique activation mechanism, further study will be required to determine how IRF3 is modified by the ANG II-Ras-ERK signaling pathway as well as the detailed molecular nature of the ANG II-stimulated active form of IRF3 and the cofactors involved. Whatever the mechanism, it is interesting that type I IFN genes are selectively induced by activated innate immune receptors but not ANG II stimulation (data not shown), while the *Cxcl10* gene is induced by both. We infer that the difference in transcriptional activity between the 2 distinct forms of activated IRF3 may be due to the promoter context in which the contribution of other, cooperating transcription factors determines the gene promoter's fate.

In summary, our present study reveals a hitherto unknown function of IRF3 in cardiac fibrosis and provides new insight into the hypertension-induced progression of cardiac remodeling. Further study on ANG II-induced IRF3 activation mechanisms may provide clinically useful information on the prevention of hypertension-associated heart failure. FJ

The authors thank A. Fukamizu (Tsukuba University, Tsukuba, Japan) for murine AT1a receptor expression vector and AT1a-293T cell line; S. Yamaoka (Tokyo Medical and Dental University, Tokyo, Japan) for Pin1 expression vector; M. Matsuda (Kyoto University, Kyoto, Japan) for RasV12 expression vector; D. Savitsky, T. Fujita, K. Maemura, K. Honda, T. Tamura, T. Suzuki, S. Kano, and H. Negishi for invaluable advice; and N. Yamanaka and M. Shishido for technical assistance. This work was supported in part by grants KAKENHI 17012005, 19041021, 19500492, and 21790710 and by the Global Center of Excellence Program Integrative Life Science Based on the Study of Biosignaling Mechanisms from the Ministry of Education, Culture, Sports, Science, and Technology of Japan.

REFERENCES

1. Kannel, W. B. (2000) Incidence and epidemiology of heart failure. *Heart Fail. Rev.* **5,** 167–173
2. Kai, H., Kuwahara, F., Tokuda, K., and Imaizumi, T. (2005) Diastolic dysfunction in hypertensive hearts: roles of perivascular inflammation and reactive myocardial fibrosis. *Hypertens. Res.* **28,** 483–490
3. Weber, K. T., Pick, R., Jalil, J. E., Janicki, J. S., and Carroll, E. P. (1989) Patterns of myocardial fibrosis. *J. Mol. Cell. Cardiol.* **21** (Suppl. 5), 121–131
4. Matsumoto, T., Wada, A., Tsutamoto, T., Ohnishi, M., Isono, T., and Kinoshita, M. (2003) Chymase inhibition prevents cardiac fibrosis and improves diastolic dysfunction in the progression of heart failure. *Circulation* **107,** 2555–2558
5. Malhotra, R., Sadoshima, J., Brosius, F. C., 3rd, and Izumo, S. (1999) Mechanical stretch and angiotensin II differentially upregulate the renin-angiotensin system in cardiac myocytes in vitro. *Circ. Res.* **85,** 137–146
6. The CONSENSUS Trial Study Group (1987) Effects of enalapril on mortality in severe congestive heart failure. Results of the Cooperative North Scandinavian Enalapril Survival Study (CONSENSUS). The CONSENSUS Trial Study Group. *N. Engl. J. Med.* **316,** 1429–1435
7. The SOLVD Investigators (1991) Effect of enalapril on survival in patients with reduced left ventricular ejection fractions and congestive heart failure. The SOLVD Investigators. *N. Engl. J. Med.* **325,** 293–302
8. Swedberg, K., Held, P., Kjekshus, J., Rasmussen, K., Ryden, L., and Wedel, H. (1992) Effects of the early administration of enalapril on mortality in patients with acute myocardial infarction. Results of the Cooperative New Scandinavian Enalapril Survival Study II (CONSENSUS II). *N. Engl. J. Med.* **327,** 678–684
9. Sano, M., Fukuda, K., Kodama, H., Pan, J., Saito, M., Matsuzaki, J., Takahashi, T., Makino, S., Kato, T., and Ogawa, S. (2000) Interleukin-6 family of cytokines mediate angiotensin II-induced cardiac hypertrophy in rodent cardiomyocytes. *J. Biol. Chem.* **275,** 29717–29723
10. Shishido, T., Nozaki, N., Yamaguchi, S., Shibata, Y., Nitobe, J., Miyamoto, T., Takahashi, H., Arimoto, T., Maeda, K., Yamakawa, M., Takeuchi, O., Akira, S., Takeishi, Y., and Kubota, I. (2003) Toll-like receptor-2 modulates ventricular remodeling after myocardial infarction. *Circulation* **108,** 2905–2910
11. Kiechl, S., Lorenz, E., Reindl, M., Wiedermann, C. J., Oberhollenzer, F., Bonora, E., Willeit, J., and Schwartz, D. A. (2002) Toll-like receptor 4 polymorphisms and atherogenesis. *N. Engl. J. Med.* **347,** 185–192
12. Tsutamoto, T., Hisanaga, T., Wada, A., Maeda, K., Ohnishi, M., Fukai, D., Mabuchi, N., Sawaki, M., and Kinoshita, M. (1998) Interleukin-6 spillover in the peripheral circulation increases with the severity of heart failure, and the high plasma level of interleukin-6 is an important prognostic predictor in patients with congestive heart failure. *J. Am. Coll. Cardiol.* **31,** 391–398
13. Vasan, R. S., Sullivan, L. M., Roubenoff, R., Dinarello, C. A., Harris, T., Benjamin, E. J., Sawyer, D. B., Levy, D., Wilson, P. W., and D'Agostino, R. B. (2003) Inflammatory markers and risk of heart failure in elderly subjects without prior myocardial infarction: the Framingham Heart Study. *Circulation* **107,** 1486–1491
14. Nakaya, T., Sato, M., Hata, N., Asagiri, M., Suemori, H., Noguchi, S., Tanaka, N., and Taniguchi, T. (2001) Gene induction pathways mediated by distinct IRFs during viral infection. *Biochem. Biophys. Res. Commun.* **283,** 1150–1156
15. Takaoka, A., Tamura, T., and Taniguchi, T. (2008) Interferon regulatory factor family of transcription factors and regulation of oncogenesis. *Cancer Sci.* **99,** 467–478
16. Sharma, S., tenOever, B. R., Grandvaux, N., Zhou, G. P., Lin, R., and Hiscott, J. (2003) Triggering the interferon antiviral response through an IKK-related pathway. *Science* **300,** 1148–1151
17. Fitzgerald, K. A., McWhirter, S. M., Faia, K. L., Rowe, D. C., Latz, E., Golenbock, D. T., Coyle, A. J., Liao, S. M., and Maniatis, T. (2003) IKKepsilon and TBK1 are essential components of the IRF3 signaling pathway. *Nat. Immunol.* **4,** 491–496
18. Honda, K., Takaoka, A., and Taniguchi, T. (2006) Type I interferon [corrected] gene induction by the interferon regulatory factor family of transcription factors. *Immunity* **25,** 349–360
19. Honda, K., and Taniguchi, T. (2006) IRFs: master regulators of signalling by Toll-like receptors and cytosolic pattern-recognition receptors. *Nat. Rev. Immunol.* **6,** 644–658
20. Sato, M., Suemori, H., Hata, N., Asagiri, M., Ogasawara, K., Nakao, K., Nakaya, T., Katsuki, M., Noguchi, S., Tanaka, N., and Taniguchi, T. (2000) Distinct and essential roles of transcription factors IRF-3 and IRF-7 in response to viruses for IFN-alpha/beta gene induction. *Immunity* **13,** 539–548
21. Mori, M., Yoneyama, M., Ito, T., Takahashi, K., Inagaki, F., and Fujita, T. (2004) Identification of Ser-386 of interferon regulatory factor 3 as critical target for inducible phosphorylation that determines activation. *J. Biol. Chem.* **279,** 9698–9702
22. Servant, M. J., ten Oever, B., LePage, C., Conti, L., Gessani, S., Julkunen, I., Lin, R., and Hiscott, J. (2001) Identification of distinct signaling pathways leading to the phosphorylation of interferon regulatory factor 3. *J. Biol. Chem.* **276,** 355–363
23. Honda, K., Yanai, H., Negishi, H., Asagiri, M., Sato, M., Mizutani, T., Shimada, N., Ohba, Y., Takaoka, A., Yoshida, N., and Taniguchi, T. (2005) IRF-7 is the master regulator of type-I interferon-dependent immune responses. *Nature* **434,** 772–777
24. Honda, K., Sakaguchi, S., Nakajima, C., Watanabe, A., Yanai, H., Matsumoto, M., Ohteki, T., Kaisho, T., Takaoka, A., Akira, S., Seya, T., and Taniguchi, T. (2003) Selective contribution of IFN-alpha/beta signaling to the maturation of dendritic cells induced by double-stranded RNA or viral infection. *Proc. Natl. Acad. Sci. U. S. A.* **100,** 10872–10877
25. Sata, M., Saiura, A., Kunisato, A., Tojo, A., Okada, S., Tokuhisa, T., Hirai, H., Makuuchi, M., Hirata, Y., and Nagai, R. (2002)

Hematopoietic stem cells differentiate into vascular cells that participate in the pathogenesis of atherosclerosis. *Nat. Med.* **8,** 403–409
26. Borgland, S. L., Bowen, G. P., Wong, N. C., Libermann, T. A., and Muruve, D. A. (2000) Adenovirus vector-induced expression of the C-X-C chemokine IP-10 is mediated through capsid-dependent activation of NF-kappaB. *J. Virol.* **74,** 3941–3947
27. Yamazaki, T., Komuro, I., Kudoh, S., Zou, Y., Nagai, R., Aikawa, R., Uozumi, H., and Yazaki, Y. (1998) Role of ion channels and exchangers in mechanical stretch-induced cardiomyocyte hypertrophy. *Circ. Res.* **82,** 430–437
28. Shindo, T., Manabe, I., Fukushima, Y., Tobe, K., Aizawa, K., Miyamoto, S., Kawai-Kowase, K., Moriyama, N., Imai, Y., Kawakami, H., Nishimatsu, H., Ishikawa, T., Suzuki, T., Morita, H., Maemura, K., Sata, M., Hirata, Y., Komukai, M., Kagechika, H., Kadowaki, T., Kurabayashi, M., and Nagai, R. (2002) Kruppel-like zinc-finger transcription factor KLF5/BTEB2 is a target for angiotensin II signaling and an essential regulator of cardiovascular remodeling. *Nat. Med.* **8,** 856–863
29. Nakajima, A., Nishimura, K., Nakaima, Y., Oh, T., Noguchi, S., Taniguchi, T., and Tamura, T. (2009) Cell type-dependent proapoptotic role of Bcl2L12 revealed by a mutation concomitant with the disruption of the juxtaposed Irf3 gene. *Proc. Natl. Acad. Sci. U. S. A.* **106,** 12448–12452
30. Liu, J. J., Li, D. L., Zhou, J., Sun, L., Zhao, M., Kong, S. S., Wang, Y. H., Yu, X. J., and Zang, W. J. (2010) Acetylcholine prevents angiotensin II-induced oxidative stress and apoptosis in H9c2 cells. [Epub ahead of print] *Apoptosis* doi: 10.1007/s10495-010-0549-x
31. Hitomi, H., Kiyomoto, H., and Nishiyama, A. (2007) Angiotensin II and oxidative stress. *Curr. Opin. Cardiol.* **22,** 311–315
32. Hoit, B. D., Shao, Y., Kinoshita, A., Gabel, M., Husain, A., and Walsh, R. A. (1995) Effects of angiotensin II generated by an angiotensin converting enzyme-independent pathway on left ventricular performance in the conscious baboon. *J. Clin. Invest.* **95,** 1519–1527
33. Lin, M., Sumimoto, T., and Hiwada, K. (1995) Left ventricular geometry and cardiac function in mild to moderate essential hypertension. *Hypertens. Res.* **18,** 151–157
34. Ogawa, S., Lozach, J., Benner, C., Pascual, G., Tangirala, R. K., Westin, S., Hoffmann, A., Subramaniam, S., David, M., Rosenfeld, M. G., and Glass, C. K. (2005) Molecular determinants of crosstalk between nuclear receptors and toll-like receptors. *Cell* **122,** 707–721
35. Moore, B. B., Murray, L., Das, A., Wilke, C. A., Herrygers, A. B., and Toews, G. B. (2006) The role of CCL12 in the recruitment of fibrocytes and lung fibrosis. *Am. J. Respir. Cell Mol. Biol.* **35,** 175–181
36. Rodriguez-Vita, J., Sanchez-Lopez, E., Esteban, V., Ruperez, M., Egido, J., and Ruiz-Ortega, M. (2005) Angiotensin II activates the Smad pathway in vascular smooth muscle cells by a transforming growth factor-beta-independent mechanism. *Circulation* **111,** 2509–2517
37. Wang, W., Huang, X. R., Canlas, E., Oka, K., Truong, L. D., Deng, C., Bhowmick, N. A., Ju, W., Bottinger, E. P., and Lan, H. Y. (2006) Essential role of Smad3 in angiotensin II-induced vascular fibrosis. *Circ. Res.* **98,** 1032–1039
38. Grande, M. T., and Lopez-Novoa, J. M. (2009) Fibroblast activation and myofibroblast generation in obstructive nephropathy. *Nat. Rev. Nephrol.* **5,** 319–328
39. Cassis, L. A., Rateri, D. L., Lu, H., and Daugherty, A. (2007) Bone marrow transplantation reveals that recipient AT1a receptors are required to initiate angiotensin II-induced atherosclerosis and aneurysms. *Arterioscler. Thromb. Vasc. Biol.* **27,** 380–386
40. Yamamoto, M., Sato, S., Mori, K., Hoshino, K., Takeuchi, O., Takeda, K., and Akira, S. (2002) Cutting edge: a novel Toll/IL-1 receptor domain-containing adapter that preferentially activates the IFN-beta promoter in the Toll-like receptor signaling. *J. Immunol.* **169,** 6668–6672
41. Ishida, J., Asada, S., Daitoku, H., Fujiwara, K., Kon, Y., Sugaya, T., Murakami, K., Nakajima, T., Kasuya, Y., and Fukamizu, A. (1999) Expression and characterization of mouse angiotensin II type 1a receptor tagging hemagglutinin epitope in cultured cells. *Int. J. Mol. Med.* **3,** 263–270
42. Touyz, R. M., and Schiffrin, E. L. (2000) Signal transduction mechanisms mediating the physiological and pathophysiological actions of angiotensin II in vascular smooth muscle cells. *Pharmacol. Rev.* **52,** 639–672
43. Sadoshima, J., and Izumo, S. (1996) The heterotrimeric G q protein-coupled angiotensin II receptor activates p21 ras via the tyrosine kinase-Shc-Grb2-Sos pathway in cardiac myocytes. *EMBO J.* **15,** 775–787
44. Deguchi, J., Makuuchi, M., Nakaoka, T., Collins, T., and Takuwa, Y. (1999) Angiotensin II stimulates platelet-derived growth factor-B chain expression in newborn rat vascular smooth muscle cells and neointimal cells through Ras, extracellular signal-regulated protein kinase, and c-Jun N-terminal protein kinase mechanisms. *Circ. Res.* **85,** 565–574
45. Seta, K., Nanamori, M., Modrall, J. G., Neubig, R. R., and Sadoshima, J. (2002) AT1 receptor mutant lacking heterotrimeric G protein coupling activates the Src-Ras-ERK pathway without nuclear translocation of ERKs. *J. Biol. Chem.* **277,** 9268–9277
46. Yoneyama, M., Suhara, W., Fukuhara, Y., Fukuda, M., Nishida, E., and Fujita, T. (1998) Direct triggering of the type I interferon system by virus infection: activation of a transcription factor complex containing IRF-3 and CBP/p300. *EMBO J.* **17,** 1087–1095
47. Saitoh, T., Tun-Kyi, A., Ryo, A., Yamamoto, M., Finn, G., Fujita, T., Akira, S., Yamamoto, N., Lu, K. P., and Yamaoka, S. (2006) Negative regulation of interferon-regulatory factor 3-dependent innate antiviral response by the prolyl isomerase Pin1. *Nat. Immunol.* **7,** 598–605
48. Rader, D. J., and Daugherty, A. (2008) Translating molecular discoveries into new therapies for atherosclerosis. *Nature* **451,** 904–913
49. Libby, P. (2002) Inflammation in atherosclerosis. *Nature* **420,** 868–874
50. Dorn, G. W., 2nd, and Force, T. (2005) Protein kinase cascades in the regulation of cardiac hypertrophy. *J. Clin. Invest.* **115,** 527–537
51. Zeisberg, E. M., Tarnavski, O., Zeisberg, M., Dorfman, A. L., McMullen, J. R., Gustafsson, E., Chandraker, A., Yuan, X., Pu, W. T., Roberts, A. B., Neilson, E. G., Sayegh, M. H., Izumo, S., and Kalluri, R. (2007) Endothelial-to-mesenchymal transition contributes to cardiac fibrosis. *Nat. Med.* **13,** 952–961
52. Bellini, A., and Mattoli, S. (2007) The role of the fibrocyte, a bone marrow-derived mesenchymal progenitor, in reactive and reparative fibroses. *Lab. Invest.* **87,** 858–870
53. Prenzel, N., Zwick, E., Daub, H., Leserer, M., Abraham, R., Wallasch, C., and Ullrich, A. (1999) EGF receptor transactivation by G-protein-coupled receptors requires metalloproteinase cleavage of proHB-EGF. *Nature* **402,** 884–888

Received for publication October 6, 2010.
Accepted for publication January 6, 2011.

Bedside Teaching

IgG4と循環器疾患

今井　靖　永井　良三

呼 吸 と 循 環
第59巻　第5号 別刷
2011年5月15日　発行

医学書院

Bedside Teaching

IgG4と循環器疾患*

今井　靖[1]　永井　良三

はじめに

免疫グロブリンIgGにはIgG1～IgG4のサブクラスがあり，IgG4はIgG全体の5～6%程度を占めるminorな存在であるが，この上昇を伴う“IgG4関連疾患”が近年着目されている．このclinical entityは，自己免疫性膵炎(autoimmune pancreatitis；AIP)において最初に提唱されたが[1]，その後，胆管(硬化性胆管炎)[2]，唾液腺(慢性硬化性唾液腺炎)[3]，後腹膜線維症[4]，肝臓疾患(炎症性偽腫瘍，慢性肝炎)[5]，肺疾患(炎症性偽腫瘍，間質性肺炎)などでもこのIgG4が関与する炎症性疾患としてとらえられるようになってきた．これらの疾患群の特徴としては血清IgG4が上昇し，成人例に広く認められ，ステロイド治療に感受性があり，他臓器のIgG4が関与する硬化性病変が認められるなどといった特徴がある[6]．IgG4関連疾患はその起源となる臓器に関係なく共通の病態生理学的特徴がある．その共通点は罹患臓器に腫瘍を思わせる腫脹性病変を呈すること，びまん性にリンパ球・形質細胞の浸潤を伴うこと，時に好酸球が集簇すること，閉塞性静脈炎を伴うことがあることなどが挙げられる．そして免疫組織学的に検討を行うとIgG4陽性の形質細胞が病変内に多数集簇している所見が認められる．このIgG4が単なる血液学的マーカーではなく，IgG4陽性形質細胞が病態形成に深く関わっていることが推察されている[7]．多くのIgG4関連疾患は分泌腺・管腔組織に認められ，例外として後腹膜や縦隔[4]などに認められる．最近ではIgG4の測定そのものが保険収載され，特に自己免疫性膵炎およびミクリッツ病の診断基準にはすでにIgG4値の測定が評価項目に加えられている．

そのようななかで心臓血管系に関しても最近，IgG4の関与が考えられる病態が報告されるようになり，にわかに注目を集めている．本稿ではこの循環器領域におけるIgG4関連疾患について概観したい．

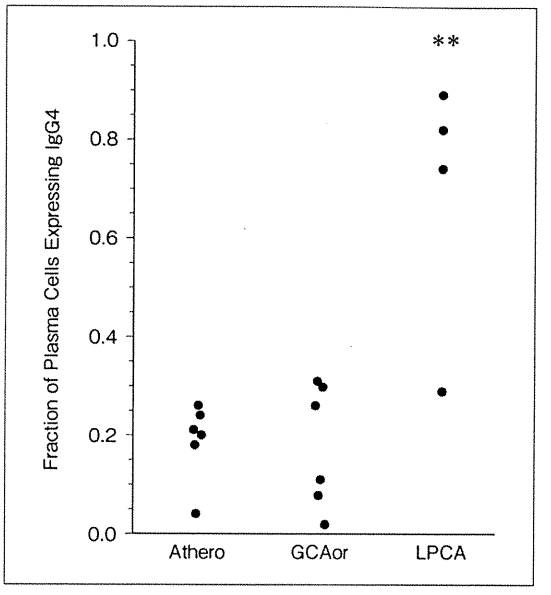

図1　Stoneらの報告
Athero：動脈硬化性，GCAor：巨細胞性血管炎，LPCA：リンパ球・形質細胞浸襲を伴う血管炎．

* IgG4-related Cardiovascular Diseases

[1] 東京大学大学院医学系研究科循環器内科(〒113-8655 東京都文京区本郷7-3-1)　Yasushi Imai, Ryozo Nagai：Department of Cardiovascular Medicine, Graduate School of Medicine, University of Tokyo

0452-3458/11/¥500/論文/JCOPY

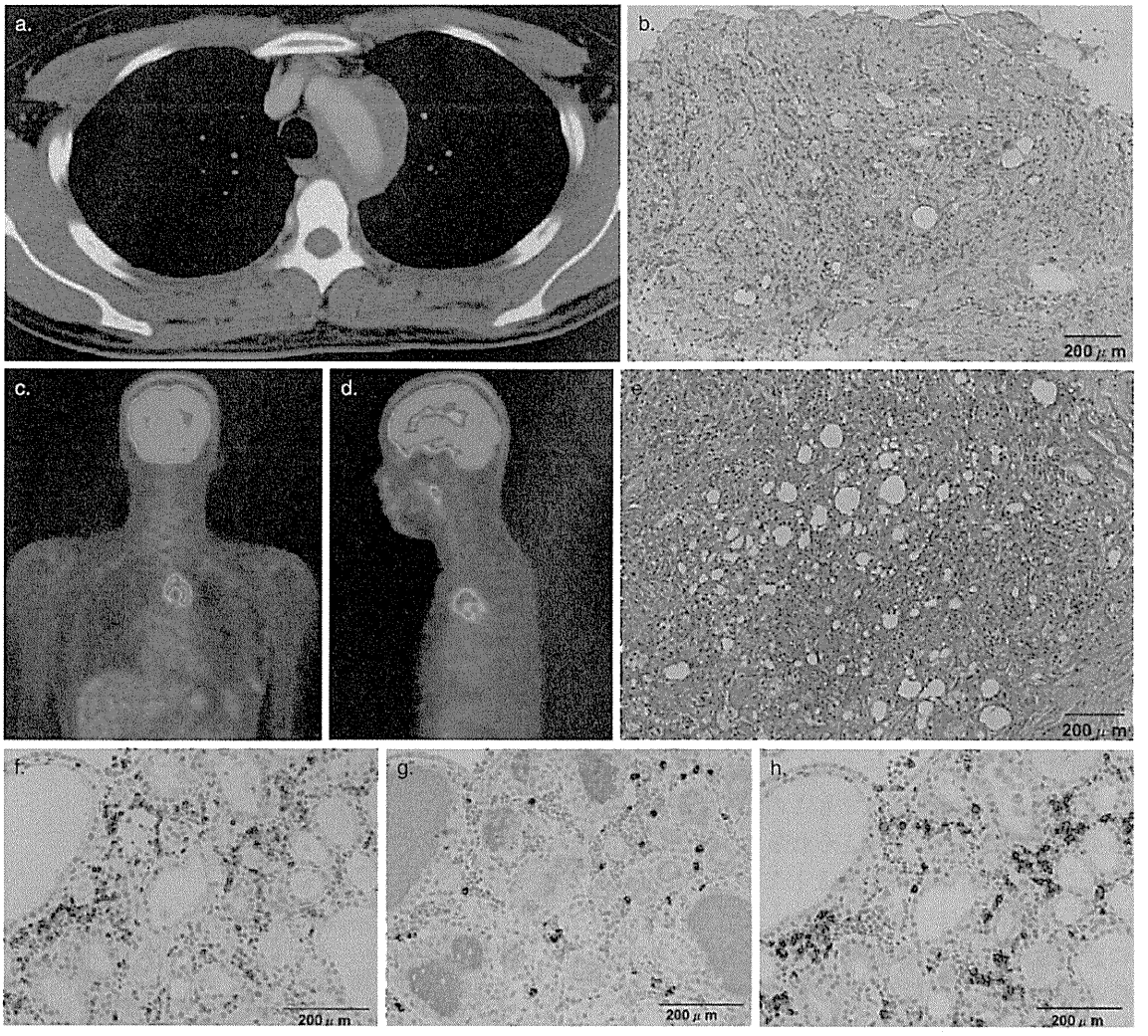

図2 大動脈周囲炎の1例(自施設)

a. 胸部CT. 大動脈弓部の顕著な肥厚がみられる. **b.** ヘマトキシリン・エオジン染色. 炎症細胞浸潤が目立つ. **c, d.** PET. 大動脈弓部への顕著な集積がみられる. **e.** エラスティカ・ワンギーソン染色. 顕著な線維化が認められる. **f.** CD3, **g.** IgG4, **h.** CD20(**f, g, h.** 免疫組織学的検討)

慢性大動脈周囲炎とIgG4関連疾患

慢性大動脈周囲炎[8~10]は大動脈や分岐周辺の炎症および線維化が強い疾患群と考えられるもので, 別の呼称としては特発性後腹膜線維症(IRPF), 炎症性腹部大動脈瘤(IAAA), 大動脈瘤周囲の後腹膜線維症(perianeurysmal RPF)の3つの疾患が該当するものと思われる. これらは組織学的に粥状動脈硬化, 中膜の菲薄化, リンパ球や形質細胞の浸潤を伴う外膜中心の炎症が主体である点などで共通点が多い. また治療においても免疫抑制剤に対する有効性も高く, 免疫の活性化の関与が強く示唆される[9, 10].

炎症性大動脈瘤[11, 12]に限定した検討になるが, 国立病院機構金沢メディカルセンターのKasashimaらが炎症性大動脈瘤を含む大動脈瘤について臨床病理学的に検討した報告[13]があり, 炎症性大動脈瘤の10例のうち4例においてIgG4陽性形

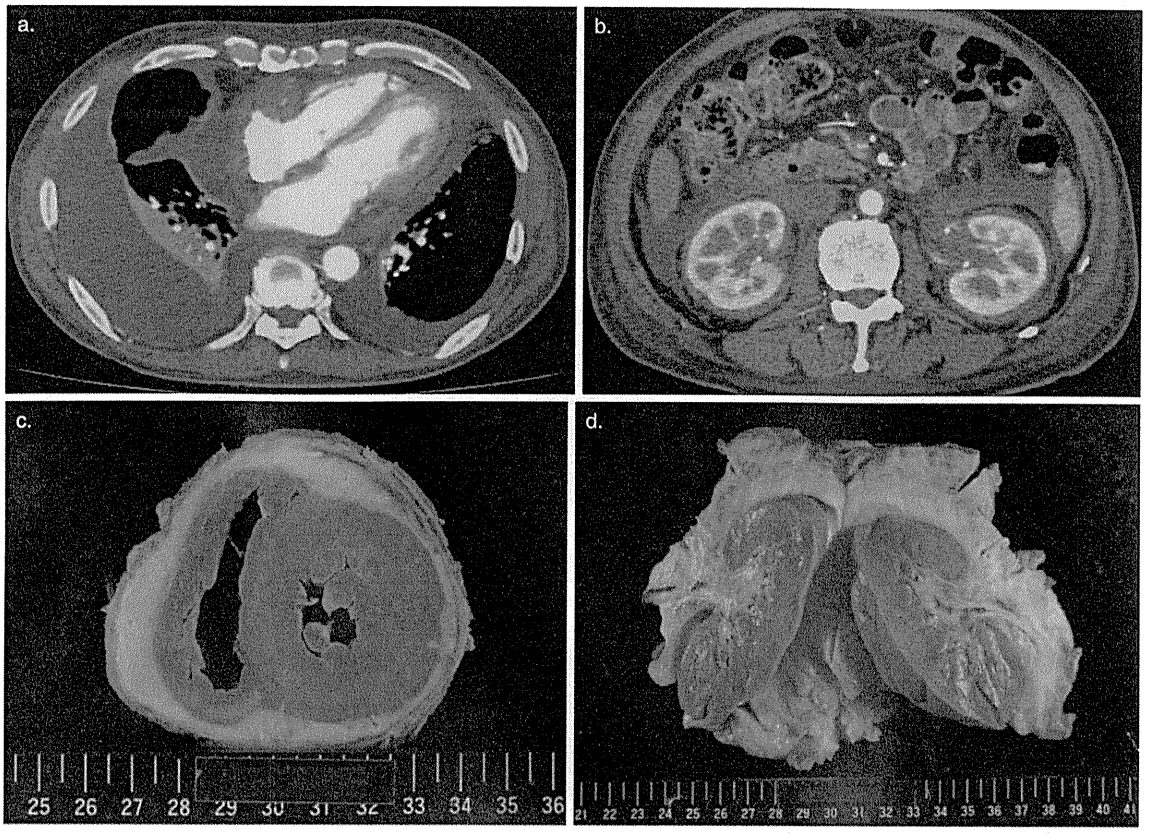

図3 後腹膜線維症・収縮性心膜炎合併例(自施設)
a, b. CT検査．心膜の肥厚に加え，大動脈壁の肥厚，腎臓周囲・後腹膜の顕著な肥厚は明らかである．
c, d. 肉眼病理所見．

質細胞が外膜にびまん性に浸潤し血清IgG4が高値を呈していたとしており，炎症性大動脈瘤の少なくとも部分的にはIgG4関連疾患が含まれることを示している．

さらに最近では海外から大規模な集団で大動脈瘤について検討された論文があり，Stoneらは病院の病理に集積された5年間の病理サンプルを用いて非感染性胸部大動脈瘤638例を調査，そのうち33例5.2%に非感染性大動脈炎の所見が認められた[14]．これらのうち4例ではリンパ球・形質細胞侵襲を伴う血管炎であり，さらにそのうち3例はIgG4関連疾患であり，免疫組織学的に評価を行うことの有用性を指摘している．また組織におけるIgG4陽性形質細胞の比率をグラフ化する(**図1**)と優位にIgG4関連疾患と考えられる血管炎でIgG4陽性形質細胞が多いことが分かる．

われわれの施設においても，このような大動脈周囲炎を数例経験しており，そのひとつは最近症例報告している[15]．31歳男性で大動脈周囲に顕著な線維性肥厚を認め，組織学的にはリンパ球，形質細胞侵襲を認め免疫組織学的にIgG4陽性細胞が多く認められた(**図2**)．また，血液生化学的に血中IgG4は263 mg/dlと有意に高値であった．18F-fluorodeoxyglucoseを用いたPETではこの領域に強い集積を認め(**図2**)，コルチコステロイド治療後はその治療効果に平行してPETの集積性が低下した．

これらの報告を含めて考察すると，大動脈疾患のなかの特に血管壁から外膜にかけて炎症の主座があるもののなかにIgG4関連疾患としての大動脈周囲炎という疾患のとらえ方が今後必要になるものと思われ，さらなるデータの集積が期待され

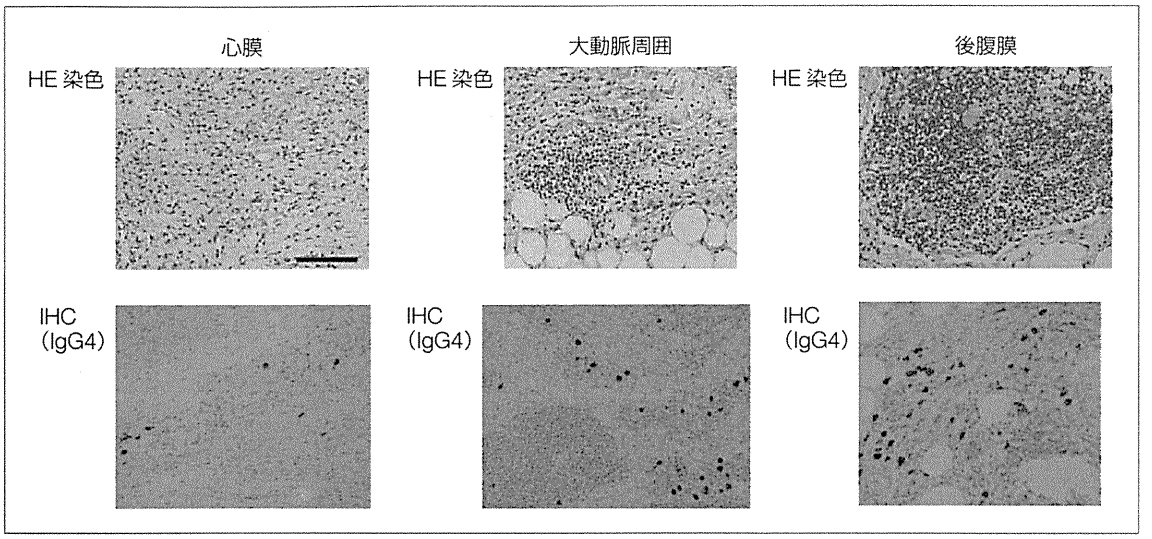

図4 顕微鏡的所見

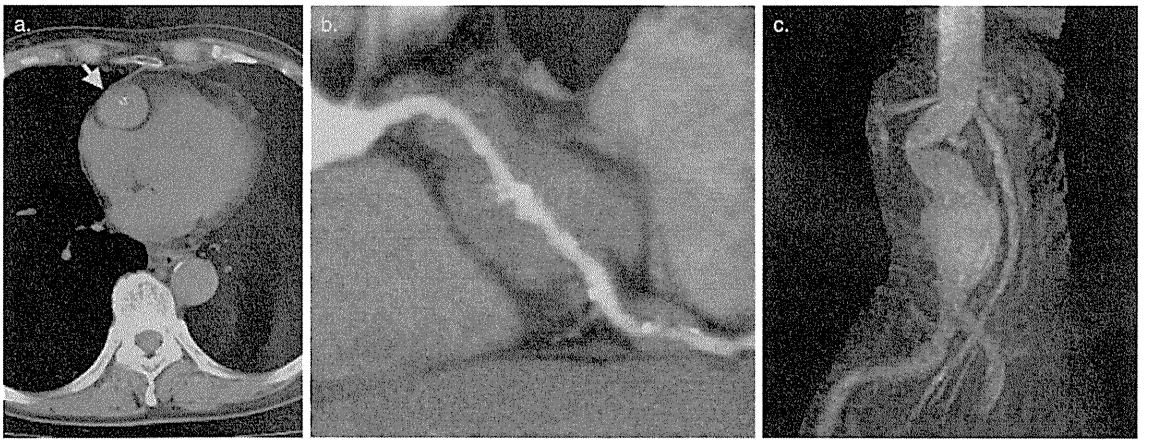

図5 冠動脈および腹部大動脈のCT所見

る．

慢性心膜炎・心タンポナーデとIgG4関連疾患

典型的なIgG4関連疾患としてわれわれが初めて経験したのは，後腹膜線維症に心膜周囲に顕著な線維性肥厚を伴う収縮性心膜炎を呈した症例であり，その症例の概要は本誌にも掲載された(**図3，4**)[16]．不幸にしてその症例は心不全の悪化・循環不全の結果，死の転帰を辿った．病理解剖の結果，心膜・後腹膜および大動脈周囲の強い線維性肥厚を認め，炎症細胞が集簇しIgG4陽性細胞が散見された(**図3，4**)．文献的にIgG4関連疾患，あるいは当疾患と関連が深い後腹膜線維症との合併による心膜炎について過去にいくつか報告が認められるが[17~20]，胸膜，大動脈周囲，他臓器などで線維性病変を伴うものが多かった．免疫抑制剤投与により心膜炎に伴う心嚢水貯留が軽減する場合が多いとされるが，しかし，収縮性心膜炎を来し，心膜切除術・心不全治療を行っても治療抵抗性で病状が進行することもあり，きめ細やかな対応が必要であるとともに，早い段階から免疫抑制剤投与を考慮する必要性がある．

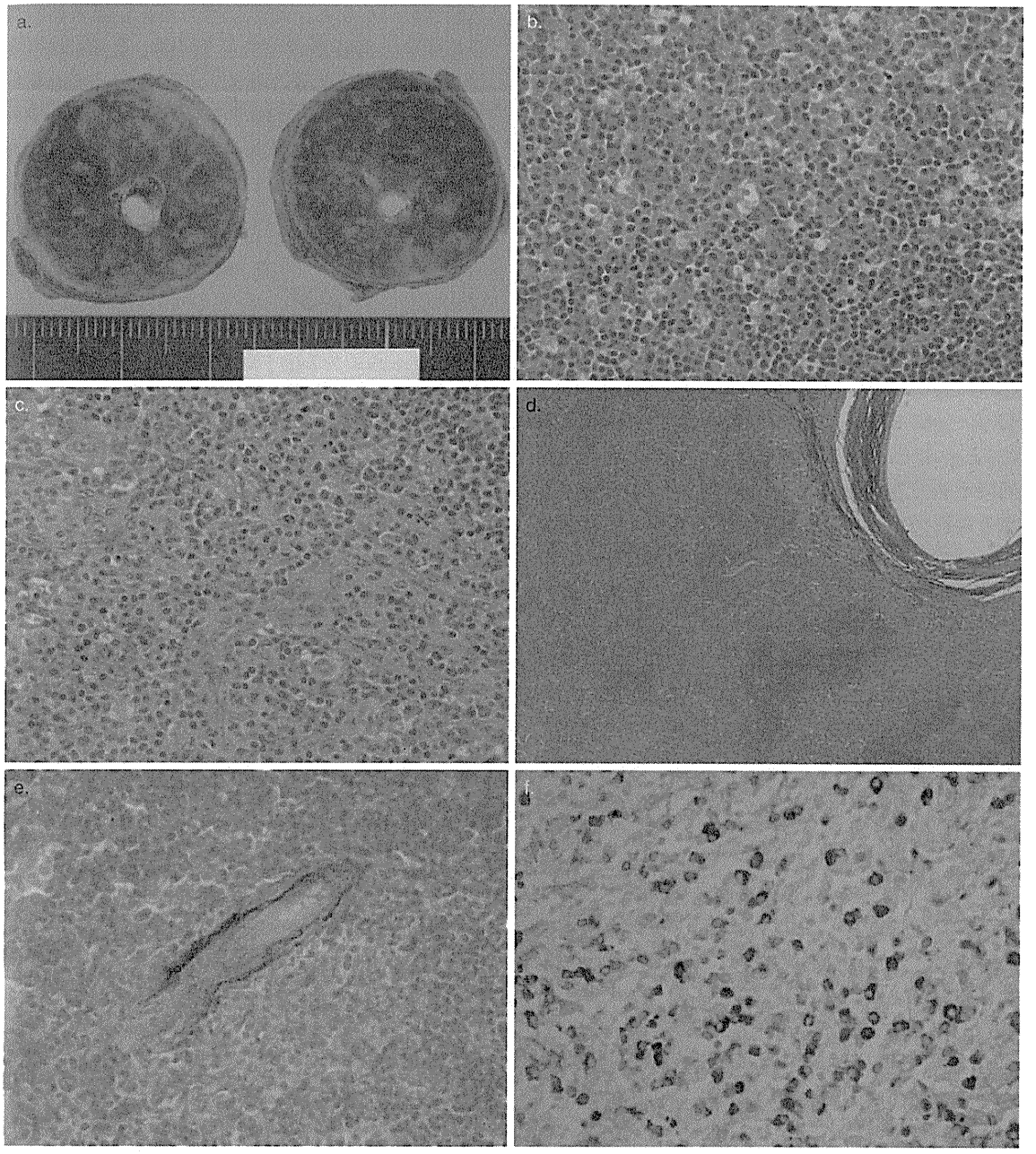

図6 手術にて摘出された冠動脈周囲炎とその顕微鏡所見
a. 右冠動脈の周囲炎の部位の断面像. **b.** HE染色. リンパ球, 形質細胞浸潤が目立つ. **c.** 好酸球が散見される. **d.** EVG染色で顕著な線維化を認める. **e.** 閉塞性静脈炎の所見を認める. **f.** 多数のIgG4陽性形質細胞を認める. (文献[21]より引用. 解説文は翻訳したものを要約した)

IgG4関連疾患としての冠動脈周囲炎

最近, 冠動脈の動脈壁周囲が顕著に肥厚する症例報告が循環器系の学会で散見されるが, 前述の金沢メディカルセンターから, 大動脈周囲炎のみならず冠動脈にも動脈周囲炎を呈した症例が報告